

Predicting the Dislocation Nucleation Rate as a Function of Temperature and Stress

Seunghwa Ryu¹, Keonwook Kang², and Wei Cai^{3*}

¹*Department of Physics, Stanford University, Stanford, California 94305, USA*

²*Theoretical Division, Los Alamos National Laboratory, Los Alamos, NM 87545, USA*

³*Department of Mechanical Engineering,
Stanford University, Stanford, California 94305, USA*

Abstract

Predicting the dislocation nucleation rate as a function of temperature and stress is crucial for understanding the plastic deformation of nanoscale crystalline materials. However, the limited time scale of molecular dynamics simulations makes it very difficult to predict dislocation nucleation rate at experimentally relevant conditions. Recently, we developed an approach to predict dislocation nucleation rate based on the Becker-Döring theory of nucleation and umbrella sampling simulations. The results reveal very large activation entropies, originated from the anharmonic effects, which can alter the nucleation rate by many orders of magnitude. Here we discuss the thermodynamics and algorithms underlying these calculations in greater detail. In particular, we prove that the activation Helmholtz free energy equals the activation Gibbs free energy in the thermodynamic limit, and explain the large difference in the activation entropies in the constant stress and constant strain ensembles. We also discuss the origin of the large activation entropies for dislocation nucleation, along with previous theoretical estimates of the activation entropy.

* Corresponding author: caiwei@stanford.edu

I. INTRODUCTION

Dislocation nucleation is essential to the understanding of ductility and plastic deformation of crystalline materials with sub-micrometer dimension¹⁻³ or under nano-indentation⁴⁻⁶, and to the synthesis of high quality thin films for microelectronic, optical and magnetic applications^{7,8}. The fundamental quantity of interest is the dislocation nucleation rate I as a function of stress σ and temperature T . Continuum⁹⁻¹¹ and atomistic models¹²⁻¹⁴ have been used to predict dislocation nucleation rate and they both have limitations. The applicability of continuum models may be questionable because the size of the critical dislocation nucleus can be as small as a few lattice spacing. In addition, the continuum models are often based on linear elasticity theory, while dislocation nucleation typically occur at high strain conditions in which the stress-strain relation becomes non-linear. These difficulties do not arise in molecular dynamics (MD) simulations, which can reveal important mechanistic details of dislocation nucleation. Unfortunately, the time step of MD simulations is on the order of a femto-second, so that the time scale of MD simulations is typically on the order of a nano-second, given existing computational resources. Therefore, the study of dislocation nucleation via direct MD simulation has been limited to extremely high strain rate ($\sim 10^8 \text{ s}^{-1}$) conditions^{12,13}. This is about 10 orders of magnitudes higher than the strain rate in most experimental work and engineering applications^{5,6}. Predicting the dislocation nucleation rate $I(\sigma, T)$ under the experimentally relevant conditions is still a major challenge.

An alternative approach is to combine reaction rate theories¹⁵⁻¹⁷ with atomistic models. Atomistic simulations can be used to compute the activation barrier, which is used as an input for the reaction rate theory to predict the dislocation nucleation rate. There are several reaction rate theories, such as the transition state theory^{15,18} and the Becker-Döring theory¹⁶, which lead to similar expressions for the nucleation rate,

$$I(\sigma, T) = N_s \nu_0 \exp \left[-\frac{G_c(\sigma, T)}{k_B T} \right] \quad (1)$$

where N_s is the number of equivalent nucleation sites, ν_0 is a frequency prefactor, G_c is the activation Gibbs free energy for dislocation nucleation, and k_B is Boltzmann's constant. The difference between the theories lie in the expression of the frequency prefactor ν_0 . In practice, ν_0 is often approximated by the Debye frequency ν_D of the crystal, which is typically on the order of 10^{13} s^{-1} . One could also express the dislocation nucleation rate as a function of

strain γ and temperature T . Then,

$$I(\gamma, T) = N_s \nu_0 \exp \left[-\frac{F_c(\gamma, T)}{k_B T} \right] \quad (2)$$

where F_c is the activation Helmholtz free energy for dislocation nucleation.

The transition state theory (TST)^{15,18} has often been combined with the nudged elastic band (NEB) method¹⁹ to predict the rate of rare events in solids^{14,20,21}. However, there exist several limitations for this approach. First, TST is known to overestimate the rate because it does not account for the fact that a single reaction trajectory may cross the saddle region multiple times. This deficiency can be corrected by introducing a recrossing factor which can be computed by running many MD simulations started from the saddle region²². A more serious problem is that the NEB method, and the closely related string method²³, only determines the activation barrier at zero temperature, i.e. $G_c(\sigma, T = 0)$ or $F_c(\gamma, T = 0)$. In principle, the activation barrier at finite temperature can be obtained from the finite-temperature string method²⁴, which has not yet been applied to dislocation nucleation. Both G_c and F_c are expected to decrease with T , as characterized by the activation entropy S_c . The effect of the activation entropy is to introduce an overall multiplicative factor of $\exp(S_c/k_B)$ to the nucleation rate (See Eq. (13)), which can be very large if S_c exceeds $10 k_B$. Until recently, the magnitude of S_c has not been determined reliably and, within the harmonic approximation of TST, S_c is estimated to be small (i.e. $\sim 3 k_B$). For example, the activation entropy of kink migration on a 30° partial dislocation in Si has recently been estimated to be less than $3 k_B$ ²¹.

Recently, we developed an approach²⁶ to accurately predict the rate $I(\sigma, T)$ of homogeneous and heterogeneous dislocation nucleation over a wide range of σ and T , based on the Becker-Döring (BD) theory¹⁶ and the umbrella sampling method²⁷. The BD theory correctly accounts for the recrossing effect, and the umbrella sampling method directly computes the activation Helmholtz free energy F_c at finite temperature. The activation Gibbs free energy $G_c(\sigma, T)$ is set to the value of $F_c(\gamma, T)$ at the strain γ that corresponds to the stress σ at temperature T . The activation entropy S_c is obtained from the reduction of G_c and F_c with temperature and is found to be very large (e.g. exceeding $9 k_B$ for $\gamma < 9\%$). Furthermore, two different activation entropies are found, depending on whether the stress or the strain is held constant when the temperature is raised. Hence the activation entropy depends on the choice of the (constant stress or constant strain) ensemble, contrary to entropy itself, which

is independent of the choice of ensemble. These effects are explained in terms of thermal expansion and thermal softening, both are anharmonic effects in the crystal.

In this paper, we provide a more thorough discussion on the thermodynamics of dislocation nucleation and algorithms underlying our approach. The thermodynamic properties of activation, such as activation free energy, activation entropy, and activation volume have been extensively discussed in the context of dislocation overcoming obstacles, using continuum theory within the constant stress ensemble²⁵. Recently, there has been interest in computing these quantities using atomistic simulations, in which it is more convenient to use the constant strain ensemble. One of the main objectives of this paper is to discuss the difference between the thermodynamic properties of activation defined in the constant stress and the constant strain ensembles in the context of dislocation nucleation. First, we prove that the activation Gibbs free energy $G_c(\sigma, T)$ equals the activation Helmholtz free energy $F_c(\gamma, T)$ for dislocation nucleation, when the volume of the crystal is much larger than the activation volume of dislocation nucleation. This leads to the intuitive conclusion that the dislocation nucleation rate is independent of whether the crystal is subjected to a constant stress or a constant strain loading condition. While the equality of $F_c(\gamma, T)$ and $G_c(\sigma, T)$ quickly leads to the difference of the two activation entropies, we provide an alternative derivation of this fact, which makes the physical origin of this difference more transparent. Our goal is to clarify why the activation entropy depend on the choice of ensemble while entropy itself does not. Second, we describe the computational methods in sufficient detail so that they can be repeated by interested readers and be adopted in their own research. We repeat our calculations using an improved order parameter to characterize dislocation nucleation and find that our previous results²⁶ are independent of the choice of order parameters, as required for self-consistency. Third, we compare our numerical results with several previous estimates of the activation entropy, such as those based on the “thermodynamic compensation law”, which states that the activation entropy is proportional to the activation enthalpy. We discuss the conditions at which this empirical law appears to hold (or fail) for dislocation nucleation.

The paper is organized as follows. Section II is devoted to the thermodynamics of dislocation nucleation. Simulation setup and computational methods are presented in Section III. Section IV presents the numerical data on activation free energy and the frequency prefactor over a wide range of stress (strain) and temperature conditions. Section V compares these

results with previous estimates of activation entropy and discusses the consequence of the activation entropy on experimentally measurable quantities, such as yield stress. This is followed by a short summary in Section VI.

II. THERMODYNAMICS OF NUCLEATION

A. Activation Free Energies

Consider a crystal of volume V subjected to stress σ at temperature T . To be specific, we can consider σ as one of the stress components, e.g. σ_{xy} , while all other stress components are zero. Let $G(n, \sigma, T)$ be the Gibbs free energy of the crystal when it contains a dislocation loop that encloses n atoms. If n is very small, the dislocation loop is more likely to shrink than to expand. On the other hand, if n is very large, the dislocation loop is more likely to expand than to shrink. There exists a critical loop size, n_c , at which the likelihood for the loop to expand equals the likelihood to shrink. It is also the loop size that maximizes the function $G(n, \sigma, T)$ for fixed σ and T . The activation Gibbs free energy is defined as,

$$G_c(\sigma, T) \equiv G(n_c, \sigma, T) - G(0, \sigma, T) \quad (3)$$

where $G(0, \sigma, T)$ is the Gibbs free energy of the perfect crystal (containing no dislocations) at stress σ and temperature T . Given $G_c(\sigma, T)$, the dislocation nucleation rate can be predicted using Eq. (1).

While experimental data are usually expressed in terms of σ and T , it is often more convenient to control strain than stress in atomistic simulations. Let γ be the strain component that corresponds to the non-zero stress component, e.g. γ_{xy} . While there is only one non-zero stress component, this usually corresponds to multiple non-zero strain components. Nonetheless, the other strain components do not appear in our discussion because their corresponding work term is zero. Thermodynamics²⁸ allows us to discuss the nucleation process within the constant γ constant T ensemble, by introducing the Helmholtz free energy $F(n, \gamma, T)$ through the Legendre transform²⁹.

$$\gamma(n, \sigma, T) \equiv -\frac{1}{V} \left. \frac{\partial G(n, \sigma, T)}{\partial \sigma} \right|_{n, T} \quad (4)$$

$$F(n, \gamma, T) \equiv G(n, \sigma, T) + \sigma \gamma V. \quad (5)$$

A convenient property of the Legendre transform is that it is reversible, i.e.,

$$\sigma(n, \gamma, T) = \frac{1}{V} \left. \frac{\partial F(n, \gamma, T)}{\partial \gamma} \right|_{n, T} \quad (6)$$

$$G(n, \sigma, T) = F(n, \gamma, T) - \sigma \gamma V. \quad (7)$$

Again, let n_c be the dislocation loop size that maximizes $F(n, \gamma, T)$ for given γ and T . In Appendix A, it is proven that the same n_c maximizes $G(n, \sigma, T)$ and $F(n, \gamma, T)$, so that the critical dislocation loop size does not depend on the choice of (constant stress or constant strain) ensemble. The activation Helmholtz free energy is defined as,

$$F_c(\gamma, T) \equiv F(n_c, \gamma, T) - F(0, \gamma, T). \quad (8)$$

Given $F_c(\gamma, T)$, the dislocation nucleation rate can be predicted using Eq. (2).

B. Activation Entropies

The activation Gibbs free energy $G_c(\sigma, T)$ decreases with increasing temperature T at fixed σ , and also decreases with increasing σ at fixed T . The activation entropy, defined as²⁵

$$S_c(\sigma, T) \equiv - \left. \frac{\partial G_c(\sigma, T)}{\partial T} \right|_{\sigma} \quad (9)$$

measures the reduction rate of $G_c(\sigma, T)$ with increasing T . Similarly, the activation volume, defined as

$$\Omega_c(\sigma, T) \equiv - \left. \frac{\partial G_c(\sigma, T)}{\partial \sigma} \right|_T \quad (10)$$

measures the reduction rate of $G_c(\sigma, T)$ with increasing σ .

The activation enthalpy H_c is defined as,

$$H_c(\sigma, T) = G_c(\sigma, T) + T S_c(\sigma, T). \quad (11)$$

The activation entropy S_c is usually insensitive to temperature, especially in the range of zero to room temperature, which will be confirmed by our numerical results. This means that H_c is also insensitive to temperature and that the Gibbs free energy can be approximated by,

$$G_c(\sigma, T) = H_c(\sigma) - T S_c(\sigma). \quad (12)$$

Consequently, the dislocation nucleation rate in Eq. (1) can be rewritten as,

$$I(\sigma, T) = N_s \nu_0 \exp\left(\frac{S_c(\sigma)}{k_B}\right) \exp\left(-\frac{H_c(\sigma)}{k_B T}\right). \quad (13)$$

Therefore, when the dislocation nucleation rate per site, I/N_s , at a constant stress σ are shown in the Arrhenius plot, e.g. Fig. 1, the data are expected to follow a straight line. The negative slope of the line can be identified as the activation enthalpy $H_c(\sigma)$ over k_B , and the intersection of the line with the vertical axis is $\nu_0 \exp(S_c(\sigma)/k_B)$. Hence the activation entropy S_c contributes an overall multiplicative factor, $\exp(S_c(\sigma)/k_B)$, to the nucleation rate. If $S_c = 3k_B$, this factor is about 20 and may be considered insignificant. However, if $S_c > 10k_B$, this factor exceeds 10^4 and cannot be ignored.

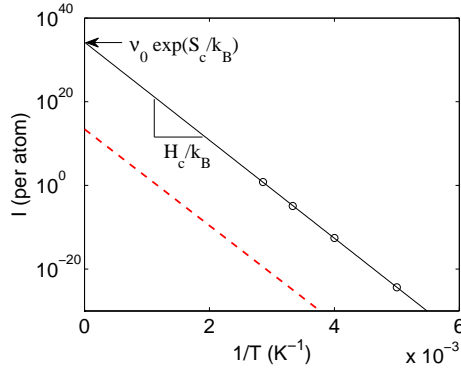


FIG. 1: Homogeneous dislocation nucleation rate per lattice site in Cu under pure shear stress $\sigma = 2.0$ GPa on the (111) plane along the $[11\bar{2}]$ direction as a function of T^{-1} , predicted by Becker-Döring theory using free energy barrier computed from umbrella sampling (See Section III). The solid line is a fit to the predicted data (in circles). The slope of the line is H_c/k_B , while the intersection point of the extrapolated line with the vertical axis is $\nu_0 \exp(S_c/k_B)$. Dashed line presents the nucleation rate predicted by $\nu_0 \exp(-H_c/k_B T)$, in which the activation entropy is completely ignored, leading to an underestimate of the nucleation rate by ~ 20 orders of magnitude.

If we choose the constant strain γ ensemble, then the focus is on the activation Helmholtz free energy $F_c(\gamma, T)$, which decreases with increasing temperature T at fixed γ . An alternative definition of the activation entropy can be given as

$$S_c(\gamma, T) \equiv - \left. \frac{\partial F_c(\gamma, T)}{\partial T} \right|_{\gamma} \quad (14)$$

which measures the reduction rate of $F_c(\gamma, T)$ with increasing T . We can then define the activation energy $E_c(\gamma, T)$ as,

$$E_c(\gamma, T) = F_c(\gamma, T) + T S_c(\gamma, T). \quad (15)$$

Again, since the activation entropy S_c is usually insensitive to temperature, we can use the following approximation for the activation Helmholtz free energy,

$$F_c(\gamma, T) = E_c(\gamma) - TS_c(\gamma). \quad (16)$$

Consequently, the dislocation nucleation rate in Eq. (2) can be rewritten as,

$$I(\gamma, T) = N_s \nu_0 \exp\left(\frac{S_c(\gamma)}{k_B}\right) \exp\left(-\frac{E_c(\gamma)}{k_B T}\right). \quad (17)$$

Therefore, $E_c(\gamma)$ and $S_c(\gamma)$ can also be identified from the slope and y -intersection in Arrhenius plot of dislocation nucleation rate at a constant strain γ .

Apparently, the above discussions in the constant σ ensemble and those in the constant γ ensemble closely resemble each other. It may seem quite natural to expect the two definition of the activation entropies, $S_c(\sigma)$ and $S_c(\gamma)$, to be one and the same, as long as σ and γ lie on the stress-strain curve of the crystal at temperature T . After all, the entropy of a crystal is a thermodynamic state variable, which is independent of whether the constant stress or constant strain ensemble is used to describe it, and we may expect the activation entropy to enjoy the same property too. Surprisingly, $S_c(\sigma)$ and $S_c(\gamma)$ are not equivalent to each other. For dislocation nucleation in a crystal, we can show that $S_c(\sigma)$ is almost always larger than $S_c(\gamma)$, and the difference between the two can be very large, e.g. $30 k_B$ for $\sigma < 2$ GPa. The large difference between the two activation entropies has not been noticed before. We will present both theoretical proofs and numerical data on this difference in subsequent sections.

C. Difference between the Two Activation Entropies

While the Gibbs free energy $G(n, \sigma, T)$ and the Helmholtz free energy $F(n, \gamma, T)$ are Legendre transforms of each other, the activation Gibbs free energy $G_c(\sigma, T)$ and the activation Helmholtz free energy $F_c(\gamma, T)$ are not Legendre transforms of each other. In fact, it is proven in Appendix B that $G_c(\sigma, T)$ and $F_c(\gamma, T)$ equal to each other, in the limit of $V \gg \Omega_c$, as long as σ and γ lie on the stress-strain curve of the perfect crystal at temperature T , i.e. $\sigma = (1/V) \partial F(0, \gamma, T) / \partial \gamma$. This has the important consequence that the dislocation nucleation rate predicted by Eq. (1) and that by Eq. (2) equal to each other. This result is intuitive because the dislocation nucleation rate should not depend on whether the crystal is subjected to a constant stress, or to a constant strain that corresponds to the same stress.

The thermodynamic properties of a crystal of macroscopic size can be equivalently specified either by its stress and temperature or by its strain and temperature, and we expect the same to hold for kinetic properties (e.g. dislocation nucleation rate) of the crystal.

It then follows that the activation entropies, $S_c(\sigma, T)$ defined in Eq. (9) and $S_c(\gamma, T)$ defined in Eq. (14), cannot equal to each other. In the following, we will let σ and γ follow the stress-strain curve, $\sigma(\gamma, T)$, of the perfect crystal at temperature T . Using the equality $G_c(\sigma, T) = F_c(\gamma, T)$, we have,

$$\begin{aligned} S_c(\sigma, T) &\equiv - \left. \frac{\partial G_c(\sigma, T)}{\partial T} \right|_{\sigma} = - \left. \frac{\partial F_c(\gamma, T)}{\partial T} \right|_{\sigma} \\ &= - \left. \frac{\partial F_c(\gamma, T)}{\partial T} \right|_{\gamma} - \left. \frac{\partial F_c(\gamma, T)}{\partial \gamma} \right|_T \left. \frac{\partial \gamma}{\partial T} \right|_{\sigma} \end{aligned} \quad (18)$$

$$= S_c(\gamma, T) - \left. \frac{\partial F_c(\gamma, T)}{\partial \gamma} \right|_T \left. \frac{\partial \gamma}{\partial T} \right|_{\sigma}. \quad (19)$$

Similarly, starting from the definition of $S_c(\gamma, T)$, we can show that,

$$S_c(\gamma, T) = S_c(\sigma, T) - \left. \frac{\partial G_c(\sigma, T)}{\partial \sigma} \right|_T \left. \frac{\partial \sigma}{\partial T} \right|_{\gamma}. \quad (20)$$

Eqs. (19) and (20) are consistent with each other because of the Maxwell relation,

$$\left. \frac{\partial \sigma}{\partial T} \right|_{\gamma} \left. \frac{\partial T}{\partial \gamma} \right|_{\sigma} \left. \frac{\partial \gamma}{\partial \sigma} \right|_T = -1 \quad (21)$$

and the chain rule of differentiation,

$$\left. \frac{\partial G_c(\sigma, T)}{\partial \sigma} \right|_T = \left. \frac{\partial F_c(\gamma, T)}{\partial \gamma} \right|_T \left. \frac{\partial \gamma}{\partial \sigma} \right|_T. \quad (22)$$

Therefore, the difference between the two activation entropies is

$$\Delta S_c \equiv S_c(\sigma, T) - S_c(\gamma, T) = \left. \frac{\partial G_c(\sigma, T)}{\partial \sigma} \right|_T \left. \frac{\partial \sigma}{\partial T} \right|_{\gamma} = - \left. \frac{\partial F_c(\gamma, T)}{\partial \gamma} \right|_T \left. \frac{\partial \gamma}{\partial T} \right|_{\sigma}. \quad (23)$$

Recall the definition of activation volume Ω_c in Eq. (10), we have

$$\Delta S_c = -\Omega_c \left. \frac{\partial \sigma}{\partial T} \right|_{\gamma}. \quad (24)$$

Notice that Ω_c is always positive and that, because of thermal softening, $\left. \frac{\partial \sigma}{\partial T} \right|_{\gamma}$ is usually negative³¹. Therefore ΔS_c is positive for dislocation nucleation in a crystal under most conditions.

While the difference between the two activation entropies have not been widely discussed, it has been pointed out by Whalley in the context of chemical reactions^{34,35}. However, ΔS_c

has been estimated to be rather small in chemical reactions. The main reason is that the activation volume for most chemical reactions is bounded. As a rough estimate, let us assume that $\Omega_c < 100\text{\AA}^3$. Under low stress conditions, we expect $\left.\frac{\partial\sigma}{\partial T}\right|_\gamma$ to be linear with stress, i.e.,

$$\left.\frac{\partial\sigma}{\partial T}\right|_\gamma \approx \frac{1}{\mu} \left.\frac{\partial\mu}{\partial T}\right|_\gamma \cdot \sigma \quad (25)$$

where μ is the shear modulus. Although for chemical reactions it is more appropriate to use the bulk modulus instead of μ , this approximation is acceptable for a rough estimate. Let us assume that μ reduces by 10% as T increases from 0 to 300 K³³, then $-\left.\frac{1}{\mu}\frac{\partial\mu}{\partial T}\right|_\gamma$ is approximately $3.3 \times 10^{-4} \text{ K}^{-1}$. If we further assume that $\sigma < 100 \text{ MPa}$, then $\Delta S_c < 0.25 k_B$, which is negligible.

The situation is quite different for dislocation nucleation, where the activation volume Ω_c diverges as σ goes to zero. The activation volume is proportional to the size n_c of the critical dislocation loop (see Appendix F). Based on a simple line tension model, it is estimated³⁶ to be $\Omega_c \propto \sigma^{-2}$ in the limit of $\sigma \rightarrow 0$. Combining this with Eq. (25), we have

$$\Delta S_c \propto \frac{1}{\mu} \left.\frac{\partial\mu}{\partial T}\right|_\gamma \cdot \sigma^{-1} \quad (26)$$

which diverges as σ goes to zero. In the relevant stress range, e.g. from 0 to 2 GPa, ΔS_c is found to be very large, easily exceeding $9 k_B$, for both homogeneous and heterogeneous dislocation nucleation, as shown in subsequent sections. The divergence of activation volume and activation entropy in the zero stress limit is a unique property of dislocation nucleation, which distinguishes itself from other thermally activated processes such as dislocation overcoming an obstacle^{37,38}.

While the expression for the difference between the two activation entropies, Eq. (24), follows mathematically from the equality of G_c and F_c and the chain rule of differentiation, one may still wonder whether there exists an alternative (perhaps more physical) explanation. After all, the entropy of the crystal is a property of the thermodynamic state and is independent of the choice of ensembles. The activation entropy can be expressed as the difference of the entropies between the “activated” state and the “initial” (i.e. meta-stable) state. It may seem puzzling that the activation entropy does not share some of the fundamental properties of entropy itself. This question is discussed in detail in Appendix C. The answer is that, in the definitions of $S_c(\sigma)$ and $S_c(\gamma)$, we are not taking the entropy difference between the same two states. If we choose the same “initial” state, then two different

“activated” states are chosen depending on whether the stress or strain is kept constant during dislocation nucleation. This is because the act of forming a critical dislocation loop introduces plastic strain into the crystal. Following this analysis, we are lead to exactly the same expression for $\Delta S_c \equiv S_c(\sigma) - S_c(\gamma)$ as Eq. (24).

A similar expression has been obtained for the difference between the point defect formation entropies under constant pressure (S_p) and under constant volume (S_v)³⁹. This difference is proportional to the relaxation volume of the defect and is negative for a vacancy and positive for an interstitial. More discussion is given in Appendix C.

D. Previous Estimates of Activation Entropy

There exist several theoretical approaches that could be used to estimate the activation entropy of dislocation nucleation. We note that none of these approaches address the fact that there are actually two different activation entropies, and, as such, they can be equally applied to $S_c(\sigma)$ and to $S_c(\gamma)$ and lead to similar estimates. In this sense, all of these approaches will lead to inconsistencies when applied to dislocation nucleation.

An approach that is widely used in the solid state is the harmonic approximation of the transition state theory (TST)¹⁵, in which the activation entropy is attributed to the vibrational degrees of freedom. In TST, the frequency prefactor is $\nu_0 = k_B T/h$ where h is Planck’s constant. At $T = 300$ K, $\nu_0 = 6.25 \times 10^{12} \text{ s}^{-1}$. Expanding the energy landscape around the “initial” state (i.e. perfect crystal, or the meta-stable state) and the “activated” state (i.e. crystal containing the critical dislocation nucleus) up to second order, we get

$$\nu_0 \exp(S_c/k_B) = \frac{\prod_{i=1}^{\mathcal{N}} \nu_i^m}{\prod_{i=1}^{\mathcal{N}-1} \nu_i^a} \quad (27)$$

where ν_i^m and ν_i^a are the positive normal frequencies in the meta-stable state and the “activated” state, respectively^{15,18,40} and \mathcal{N} is the number of normal modes in the meta-stable state. Note that the “activated” state contains one fewer normal frequency than the meta-stable state. A further (rather crude) approximation is often invoked, in which it is assumed that the normal frequencies in the “activated” state are not significantly changed from those in the meta-stable state and approximate the entire expression in Eq. (27) by the Debye frequency ν_D of the perfect crystal. The Debye frequency⁴¹ is typically the highest vibrational frequency in a crystal and is on the order of 10^{13} s^{-1} . Recall that ν_0 itself is also on the

order of 10^{13} s^{-1} at room temperature. This leads to the conclusion that $\exp(S_c/k_B)$ would not deviate from 1 by more than one order of magnitude. This is perhaps one of the reasons for the entropic effects to be largely ignored so far for dislocation nucleation processes. In subsequent sections, we will show that the activation entropies are large for dislocation nucleation and they originate from anharmonic effects. This is consistent with the above estimate that the vibrational entropy, captured by the harmonic approximation, makes a negligible contribution to the activation entropy for dislocation nucleation in metals.

Alternatively, one can estimate the activation entropy by postulating that the activation Gibbs free energy scales with the shear modulus μ of the crystal. Because μ decreases with temperature due to the thermal softening effect, so does $G_c(\sigma, T)$, leading to an activation entropy^{25,42}. This approximation can be expressed more explicitly as,

$$G_c(\sigma, T) = H_c(\sigma) \frac{\mu(T)}{\mu(0)} \quad (28)$$

where $\mu(T)$ and $\mu(0)$ are the shear moduli of the crystal at temperature T and zero temperature, respectively. Assuming that $\mu(T)$ is a linear function of T , we arrive at the following estimate for $S_c(\sigma)$,

$$S_c(\sigma) = -H_c(\sigma) \frac{1}{\mu(0)} \frac{\partial \mu}{\partial T}. \quad (29)$$

A similar expression has been derived for dislocations overcoming obstacles^{43,44}. Note that $\frac{1}{\mu(0)} \frac{\partial \mu}{\partial T}$ is a material constant that measures the severity of the thermal softening effect. For convenience, we can define a characteristic temperature T^* such that,

$$\frac{1}{T^*} = -\frac{1}{\mu(0)} \frac{\partial \mu}{\partial T} \quad (30)$$

Then we arrive at the following estimate of $S_c(\sigma)$,

$$S_c(\sigma) = \frac{H_c(\sigma)}{T^*} \quad (31)$$

Again, if we assume μ reduces by about 10% as T increases from 0 to 300 K, then $T^* \approx 3000$ K. This means $S_c(\sigma) \approx 7.5 k_B$ when $H_c(\sigma) = 2$ eV.

While the above analysis seems quite reasonable, the same argument can be applied to the activation Helmholtz free energy, leading to the following approximations,

$$F_c(\gamma, T) = E_c(\gamma) \frac{\mu(T)}{\mu(0)} \quad (32)$$

$$S_c(\gamma) = \frac{E_c(\gamma)}{T^*} \quad (33)$$

with the same T^* as defined in Eq. (30). Again, assuming $T^* \approx 3000$ K, we have $S_c(\gamma) \approx 7.5 k_B$ when $E_c(\gamma) = 2$ eV. Given the large difference between $S_c(\sigma)$ and $S_c(\gamma)$, the above two estimates cannot be both correct. In Section IV we will see that this estimate is closer to $S_c(\gamma)$ than $S_c(\sigma)$ for homogeneous dislocation nucleation in Cu.

Recently, Zhu et al.¹⁴ introduced the following approximation to the activation Gibbs free energy for dislocation nucleation from the surface of a Cu nanorod,

$$G_c(\sigma, T) = H_c(\sigma) \left(1 - \frac{T}{T_m} \right) \quad (34)$$

where T_m is the surface melting temperature of the nanorod and is chosen to be 700 K. This approximation was based on the so-called “thermodynamic compensation law”⁴⁵, or the Meyer-Neldel rule⁴⁶, which is an empirical observation that in many thermally activated processes, S_c is proportional to H_c . It is interesting that such an approximation leads to an expression for the activation entropy $S_c(\sigma)$ that is identical to Eq. (31) provided that $T^* = T_m$. This amounts to assuming that the shear modulus decreases at a constant rate with temperature and vanishes at melting temperature, as in Born’s theory of melting⁴⁷.

Again, while this approximation seems reasonable, the same argument can be applied to the activation Helmholtz free energy,

$$F_c(\gamma, T) = E_c(\gamma) \left(1 - \frac{T}{T_m} \right) \quad (35)$$

which has been used by Brochard et al.⁴⁸ This would lead to an expression for the activation entropy $S_c(\gamma)$ that is identical to Eq. (33) provided that $T^* = T_m$. Clearly, these two approximations, i.e. Eqs. (34-35), cannot both be correct, at least for the same T_m .

III. COMPUTATIONAL METHODS

A. Simulation Cell

We study both the homogeneous nucleation of dislocation in bulk Cu and the heterogeneous nucleation in a Cu nanorod. Although dislocations often nucleate heterogeneously at surfaces or internal interfaces, homogeneous nucleation is believed to occur in nano-indentation⁴ and in a model of brittle-ductile transition⁴⁹. It also provides an upper bound to the shear strength of the crystal. For simplicity, we benchmark the computational method

against brute force MD simulation and spend most of the discussions on homogeneous nucleation. Heterogeneous nucleation will be discussed following the homogeneous nucleation analysis.

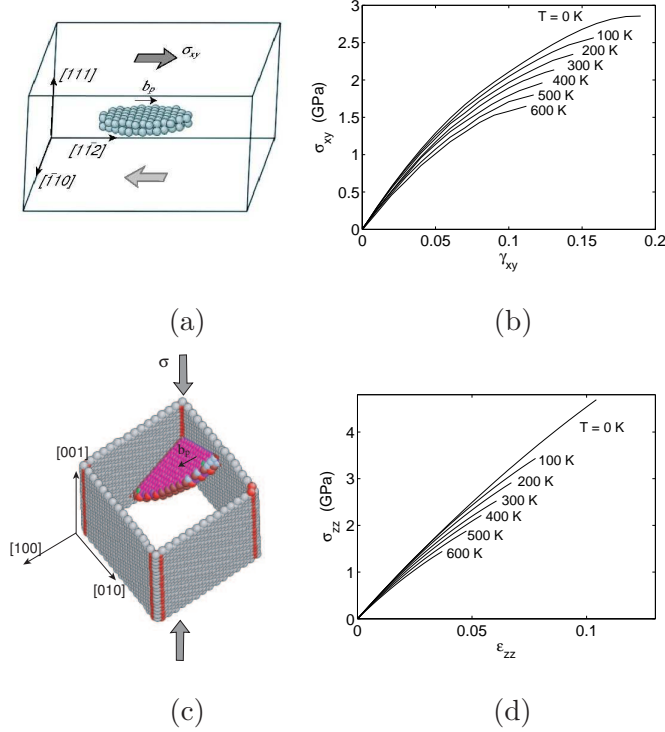


FIG. 2: Schematics of simulation cells designed for studying (a) homogeneous and (c) heterogeneous nucleation. In (a), the spheres represent atoms enclosed by the critical nucleus of a Shockley partial dislocation loop. In (c), atoms on the surface are colored by gray and atoms enclosed by the dislocation loop are colored by magenta. Shear stress-strain curves of the Cu perfect crystal (before dislocation nucleation) at different temperatures for (b) homogeneous and (d) heterogeneous nucleation simulation cells.

Our model system is a Cu single crystal described by the embedded atom method (EAM) potential⁵⁰. As shown in Fig. 2 (a), the simulation cell to study homogeneous dislocation is subjected to a pure shear stress along $[11\bar{2}]$. The dislocation to be nucleated lies on the (111) plane and has the Burgers vector of a Shockley partial⁵¹, $\vec{b}_p = [11\bar{2}]/6$. The cell has dimension of 8 repeat distances along the $[11\bar{2}]$ direction, 6 repeat distances along the $[111]$ and 3 repeat distances along the $[\bar{1}10]$, and consists of 14,976 atoms. Periodic boundary conditions (PBC) are applied to all three directions. To reduce artifacts from periodic image

interactions, the applied stress is always large enough so that the diameter of the critical dislocation loop is smaller than half the width of the simulation cell.

Fig. 2 (b) shows the shear stress strain relationship of the perfect crystal at different temperatures (before dislocation nucleation) that clearly shows the thermal softening effect. The shear strain γ is the xy component of the engineering strain. The following procedure is used to obtain the pure shear stress-strain curve, because the conventional Parrinello-Raman stress control algorithm⁵² does not work properly here due to the non-linear stress-strain relationship at large strain. At each temperature T and shear strain γ_{xy} , a series of 2 ps MD simulations under the canonical, constant temperature-constant volume (NVT) ensemble are performed. After each simulation, all strain components except γ_{xy} are adjusted according to the average Virial stress until σ_{xy} is the only nonzero stress component. The shear strain is then increased by 0.01 and the process repeats until the crystal collapses spontaneously.

For heterogeneous dislocation nucleation, we study a Cu nanorod that has the dimension of $15[100] \times 15[010] \times 20[001]$ with PBC along $[001]$, which is shown in Fig. 2 (c). When subjected to axial compression along $[001]$, a dislocation with the Burgers vector $\vec{b} = [11\bar{2}]/6$ is expected to nucleate from the corner of the nanorod. The compressive stress-strain curve is shown in Fig. 2 (d). An important step in obtaining the stress-strain curve is to achieve thermal equilibrium before taking the average of stress σ_{zz} and computing the nucleation rate at a given strain ϵ_{zz} . Due to the free side surfaces, a nano-rod undergoes low frequency but long-lived oscillations in the x and y directions (i.e. “breathing” mode) at the initial stage of MD simulation. This leads to very large oscillation in σ_{zz} , at a frequency that is several orders of magnitudes smaller than the Debye frequency. We suppress this “breath” mode by running simulation using a stochastic thermostat⁵³, which is more effective than the Nosé-Hoover thermostat⁵⁴ for equilibrating systems with a wide range of eigenfrequencies.

B. Nucleation Rate Calculation

In this work, we predict the nucleation rate based on the BD theory, which expresses the nucleation rate as

$$I^{BD}(\gamma, T) = N_s f_c^+ \Gamma \exp \left[-\frac{F_c(\gamma, T)}{k_B T} \right] \quad (36)$$

where f_c^+ is the molecular attachment rate, and Γ is the Zeldovich factor. F_c is computed with the shape and volume of the simulation cell fixed. We assume that the activation

Helmholtz free energy F_c obtained from the finite simulation cell is very close to the value of F_c in the infinite volume limit, which equals the activation Gibbs free energy G_c ⁵⁵ (see Appendix B). The BD theory and TST only differs in the frequency prefactor. Whereas TST neglects multiple recrossing over the saddle point^{15,22} by a single transition trajectory, the recrossing is accounted for in the BD theory through the Zeldovich factor.

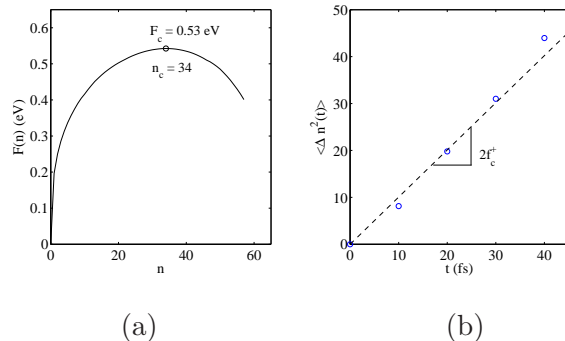


FIG. 3: (a) The Helmholtz free energy of the dislocation loop as a function of its size n during homogeneous nucleation at $T = 300$ K, $\sigma_{xy} = 2.16$ GPa ($\gamma_{xy} = 0.135$) obtained from umbrella sampling. (b) Size fluctuation of critical nuclei from MD simulations.

The Helmholtz free energy barrier F_c is computed by umbrella sampling²⁷. The umbrella sampling is performed in Monte Carlo simulations using a bias potential that is a function of the order parameter n , which is chosen to be number of atoms inside the dislocation loop. The bias potential $k_B \hat{T} (n - \bar{n})^2$ is super-imposed on the EAM potential, where $\hat{T} = 40$ K and \bar{n} is the center of the sampling window. We chose \hat{T} empirically so that the width of the sampling window on the n -axis would be about 10. The umbrella sampling provides $F(n)$ at a given γ and T . The maximum value of the free energy curve $F(n)$ is the activation free energy F_c and the maximizer is the critical dislocation loop size n_c . The Zeldovich factor Γ can be computed from the definition $\Gamma \equiv \left(\frac{\eta}{2\pi k_B T} \right)^{1/2}$, where $\eta = -\partial^2 F(n) / \partial n^2 |_{n=n_c}$.

In the previous study, we used a method suggested by Ngan et al.⁵⁷ to identify the formation of dislocation loop and compute the reaction coordinate n . We labelled an atom as “slipped” if its distance from any of its original nearest neighbors has changed by more than a critical distance d_c . We chose $d_c = 0.33, 0.38,$ and 0.43 \AA for $T \leq 400$ K, $T = 500$ K, and $T = 600$ K, respectively, because thermal fluctuation increases with temperature. The “slipped” atoms are grouped into clusters; two atoms belong to the same cluster if their

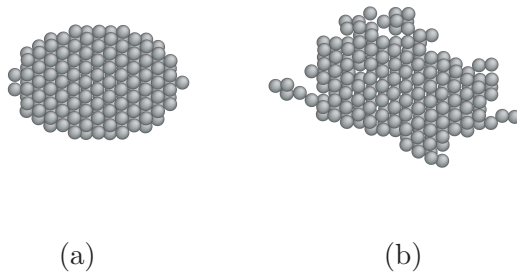


FIG. 4: Atomistic configurations of dislocation loops at (a) 0 K and (b) 300 K.

distance was less than a cutoff distance r_c (3.4\AA). The reaction coordinate is defined as the number of atoms in the largest cluster divided by two.

A possible problem of this reaction coordinate is that it does not take the slip direction into account even though we are specifically interested in slip along the $[11\bar{2}]$ direction, which is parallel to the Burgers vector of the Shockley partial. In this paper, we use another order parameter to focus exclusively on the slip along the $[11\bar{2}]$ direction. As a self-consistency check, the activation free energy should be independent of this modification of the order parameter. To compute the new order parameter during umbrella sampling, we focus on atoms on one (111) plane, each of which has 12 neighbor atoms; three in the plane above, six in the same plane, and three in the plane below. When the relative displacement along the $[11\bar{2}]$ direction between an atom and the center of mass position of its three neighbor atoms in the plane below exceeds a critical distance $d_c = 0.35\text{\AA}$, we label the atom as “slipped”. Here, we used a smaller cutoff radius of $r_c = 3.09\text{\AA}$ to group “slipped” atoms into a cluster. The size of the largest cluster of the slipped atoms is the reaction coordinate n .

As expected, we find that predictions of free energy barrier and nucleation rate are independent of these two choices of the reaction coordinate. The data obtained from these two methods match within statistical errors. In the following analysis, we will use the data from the new order parameter, because its definition appears to be more physical. Fig. 4 (a) and Fig. 4 (b) shows the critical cluster sampled by the simulation of homogeneous dislocation nucleation at $T = 0$ K (from the string method) and $T = 300$ K (from umbrella sampling), respectively. Although the dislocation loop at 0 K appears symmetric, the configuration at 300 K is distorted due to thermal fluctuation.

The attachment rate f_c^+ is computed by direct MD simulations. From umbrella sampling,

we collected an ensemble of 500 atomic configurations for which $n = n_c$, and ran MD simulations using each configuration as an initial condition. The initial velocities are randomized according to the Maxwell-Boltzmann distribution. The mean square change of the loop size, $\langle \Delta n^2(t) \rangle$, as shown in Fig. 3 (b), is fitted to a straight line⁵⁹, $2f_c^+t$, in order to extract f_c^+ .

IV. RESULTS

A. Benchmark with MD Simulations

Before applying the BD theory to predict the nucleation rate at a wide range of applied load and temperature, we would like to establish the applicability of the theory to dislocation nucleation. We benchmark the prediction of BD theory against direct MD simulations at a relatively high stress $\sigma = 2.16$ GPa ($\gamma = 0.135$) at $T = 300$ K for homogeneous nucleation. To obtain average nucleation time at the given condition, we performed 192 independent MD simulations using the NVT ensemble with random initial velocities. Each simulation ran for 4 ns. If dislocation nucleation occurred during this period, the nucleation time was recorded. This information is used to construct the function $P_s(t)$, which is the fraction of MD simulation cells in which dislocation nucleation has not occurred at time t , as shown in Fig. 5. $P_s(t)$ can be well fitted to the form of $\exp(-I^{\text{MD}}t)$, from which the nucleation rate I^{MD} is predicted to be $I^{\text{MD}} = 2.5 \times 10^8 \text{ s}^{-1}$.

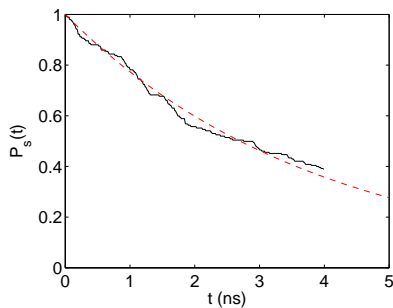


FIG. 5: The fraction of 192 MD simulations in which dislocation nucleation has not occurred at time t , $P_s(t)$, at $T = 300$ K and $\sigma_{xy} = 2.16$ GPa ($\gamma_{xy} = 0.135$). Dotted curve presents the fitted curve $\exp(-I^{\text{MD}}t)$ with $I^{\text{MD}} = 2.5 \times 10^8 \text{ s}^{-1}$.

From umbrella sampling at the specified condition, we obtain the free energy function

$F(n)$. Fig. 3 (a) shows the maximum of $F(n)$, which gives the activation free energy $F_c = 0.53 \pm 0.01$ eV and the critical nucleus size $n_c = 34$. The Zeldovich factor, $\Gamma = 0.051$, is obtained from $\Gamma \equiv \left(\frac{\eta}{2\pi k_B T}\right)^{1/2}$, where $\eta = -\partial^2 F(n)/\partial n^2|_{n=n_c}$. Using the configurations collected from umbrella sampling with $n = n_c$ as initial conditions, MD simulations give the attachment rate $f_c^+ = 5.0 \times 10^{14} \text{ s}^{-1}$, as shown in Fig. 3 (b). Because the entire crystal is subjected to uniform stress, the number of nucleation sites is the total number of atoms, $N_s = 14,976$.

Combining these data, the classical nucleation theory predicts the homogeneous dislocation nucleation rate to be $I^{\text{BD}} = 4.8 \times 10^8 \text{ s}^{-1}$, which is within a factor of two of the MD prediction. The difference between two is comparable to our error bar. This agreement is noteworthy because no adjustable parameters such as the frequency prefactor is involved in this comparison. It shows that the classical nucleation theory and our numerical approach are suitable for the calculation of the dislocation nucleation rate.

B. Homogeneous Dislocation Nucleation in Bulk Cu

Having established the applicability of nucleation theory, we now examine the homogeneous dislocation nucleation rate under a wide range of temperature and strain (stress) conditions relevant for experiments and beyond the limited timescale of brute force MD simulations. We find that the prefactor $\nu_0 = \Gamma f_c^+$ is a slowly changing function of stress and temperature. It varies by less than a factor of two for all the conditions tested here. The average value of ν_0 is about $2.5 \times 10^{13} \text{ s}^{-1}$, which is comparable to the Debye frequency $\sim 10^{13} \text{ s}^{-1}$.

The nucleation rate varies dominantly by the change of the activation free energy $F_c(\gamma, T)$, which is presented as a function of γ at different T in Fig. 6 (a). The zero temperature data (i.e. activation energies) are obtained from minimum energy path (MEP) searches using a modified version of the string method, similar to that used in the literature^{14,58}. The downward shift of F_c curves with increasing T is the signature of the activation entropy $S_c(\gamma)$. Fig. 6 (c) plots F_c as a function of T at $\gamma = 0.092$. For $T < 400$ K, the data closely follow a straight line, whose average slope gives $\overline{S_c} = 9 k_B$ in the range of $[0, 300]$ K. This activation entropy contributes a significant multiplicative factor, $\exp(S_c/k_B) \approx 10^4$, to the absolute nucleation rate, and cannot be ignored.

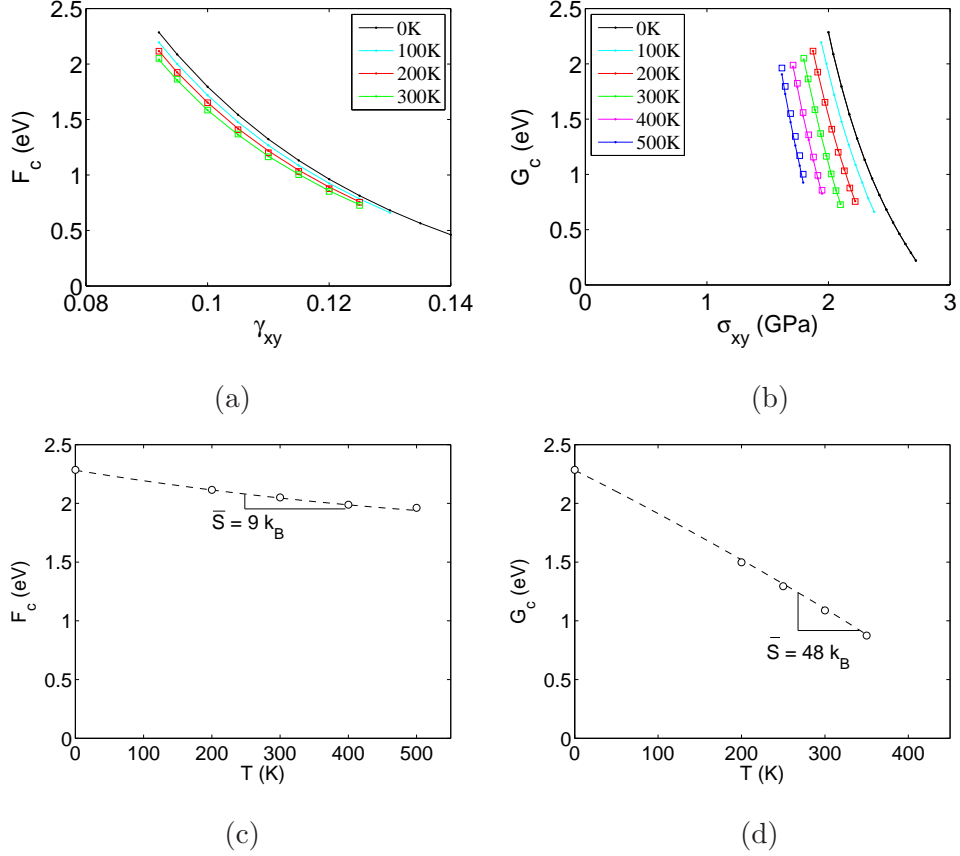


FIG. 6: Activation Helmholtz free energy for homogeneous dislocation nucleation in Cu. (a) F_c as a function of shear strain γ at different T . (b) G_c as a function of shear strain σ at different T . Squares represent umbrella sampling data and dots represent zero temperature MEP search results using simulation cells equilibrated at different temperatures. (c) F_c as a function of T at $\gamma = 0.092$. (d) G_c as a function of T at $\sigma = 2.0$ GPa. Circles represent umbrella sampling data and dashed lines represent a polynomial fit.

In Section IID, we mentioned that the activation entropy would be negligible if only the vibrational entropy were taken into account. It is likely that the origin of the large activation entropy is an anharmonic effect such as thermal expansion. To examine the effect of thermal expansion, we performed a zero temperature MEP search at $\gamma = 0.092$, but with other strain components fixed at the equilibrated values at $T = 300$ K. This approach is similar to the quasi-harmonic approximation (QHA)^{60,61} often used in free energy calculations in solids, except that, unlike QHA, the vibrational entropy is completely excluded here. The resulting activation energy, $\tilde{E}_c = 2.04$ eV, is indistinguishable from the activation free energy

$F_c = 2.05 \pm 0.01$ eV at $T = 300$ K computed from umbrella sampling. For $T < 400$ K, we observe that the activation energy \tilde{E}_c and F_c matches well at each γ and T condition (See Table I in Appendix E).

Because atoms do not vibrate in the MEP search, this result shows that the dominant mechanism for the large $S_c(\gamma)$ is indeed thermal expansion, whereas the contribution from vibrational entropy is negligible. As temperature increases, thermal expansion pushes neighboring atoms further apart and weakens their mutual interaction. This expansion makes crystallographic planes easier to shear and significantly reduces the free energy barrier for dislocation nucleation. Here, we confirm that $S_c(\gamma)$ arises almost entirely from the anharmonic effect for dislocation nucleation. At $T = 400$ K and $T = 500$ K, we observe significant differences between F_c computed from umbrella sampling and \tilde{E}_c computed from a zero temperature MEP search in expanded cell. These differences must also be attributed to anharmonic effects. The activation energy \tilde{E}_c from the expanded cell and the activation free energy $F_c(\gamma, T)$ at $T = 400$ K and $T = 500$ K are not plotted in Fig 6 (a), because they overlap with data points at lower temperatures. All data can be found in Table I in Appendix E.

Combining the activation Helmholtz free energy $F_c(\gamma, T)$ and the stress-strain relations, we obtain the activation Gibbs free energy $G_c(\sigma, T)$ shown in Fig. 6 (b). We immediately notice that the curves at different temperatures are more widely apart in $G_c(\sigma, T)$ than those in $F_c(\gamma, T)$, indicating a much larger activation entropy in the constant stress ensemble. For example, Fig. 6 (d) plots G_c as a function of T at $\sigma = 2.0$ GPa, from which we can obtain an averaged activation entropy of $\overline{S}_c(\sigma) = 48k_B$ in the temperature range of $[0, 300]$ K. This activation entropy contributes a multiplicative factor of $\exp[\overline{S}_c(\sigma)/k_B] \approx 10^{20}$ to the absolute nucleation rate, as shown in Fig. 1.

The dramatic increases in the activation entropy when stress, instead of strain, is kept constant is consistent with the theoretical prediction in Section II. This is caused by changing stress-strain relationship with temperature. For example, when the shear stress is kept at $\sigma_{xy} = 2.0$ GPa, the corresponding shear strain at $T = 0$ K is $\gamma_{xy} = 0.092$. But at $T = 300$ K, the same stress is able to cause a larger strain, $\gamma_{xy} = 0.113$. Hence at constant stress the activation free energy decreases much faster with temperature than that at constant strain.

C. Heterogeneous Dislocation Nucleation in Cu Nano-Rod

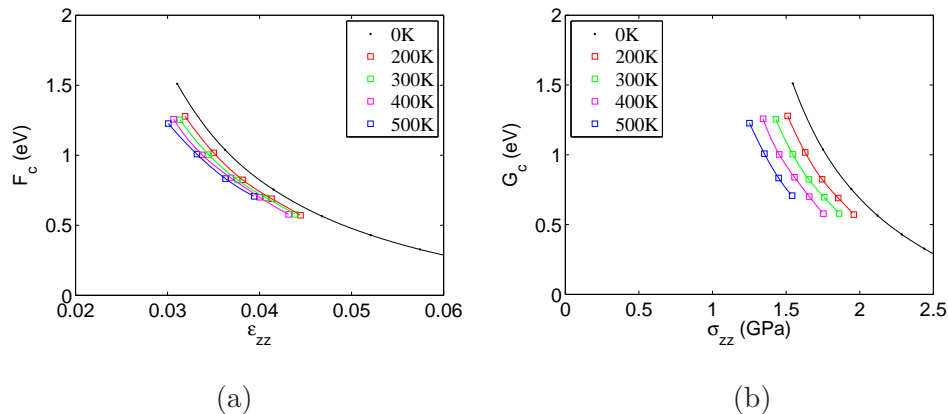


FIG. 7: Activation free energy for heterogeneous dislocation nucleation from the surface of a Cu nanorod. (a) F_c as a function of compressive strain ϵ_{zz} at different T . (b) G_c as a function of compressive stress σ_{zz} at different T . Squares represent umbrella sampling data and dots represent zero temperature MEP search results.

We studied dislocation nucleation from the corner of a [001]-oriented copper nanorod with {100} side surfaces under axial compression. While the size of dislocation loop n is the only order parameter used in the umbrella sampling, the umbrella sampling simulation automatically locates the dislocation nucleus at the corner of nanorod, as shown in Fig. 2 (c). This is because the nucleation barrier is much smaller for the nucleation from the corner than the surface, as found by Zhu et al.¹⁴ We also find that the prefactor ν_0 varies slowly similar to the case of homogeneous nucleation, changing less than one order of magnitude at all γ and T conditions tested. Interestingly, the average value of ν_0 is about $0.5 \times 10^{13} \text{ s}^{-1}$, several times smaller than the average prefactor homogeneous nucleation. The measured growth rate f_c^+ of a critical nucleus turns out to be significantly smaller (by about a factor of 3) due to the shorter dislocation line length relative to that of the complete dislocation loop in homogeneous nucleation.

Fig. 7 plots the activation free energy barrier as a function of axial compressive strain ϵ_{zz} and compressive stress σ_{zz} . Both Fig. 7 (a) and (b) show the reduction of the activation free energy with temperature, and the reduction in (b) is more pronounced due to thermal softening. For example, at the compressive elastic strain of $\epsilon = 0.03$, the compressive stress

is $\sigma = 1.56$ GPa at $T = 0$ K. The activation entropy $S_c(\epsilon)$ at this elastic strain equals $9 k_B$, whereas the activation entropy $S_c(\sigma)$ at this stress equals $17 k_B$. Unfortunately, we could not perform the minimum energy path search at zero temperature using an expanded cell to mimic the thermal expansion effect due to the free surface of the nanorod.

The activation entropy difference is smaller than the homogeneous nucleation because both thermal softening and activation volume are smaller. In order for the homogeneous nucleation to occur at room temperature, the perfect crystal must be sheared significantly, close to the ideal shear strength. In such a high non-linear elastic regime, the thermal softening effect becomes very large, as depicted in Fig. 2. However, the heterogeneous nucleation is much easier to occur so that it can happen when the nanorod is subjected to a moderate loading in which the stress-strain relation is still relatively linear. Therefore, the thermal softening effect is not as large as the case of homogeneous nucleation. Secondly, because the applied compression stress is not parallel to the slip direction (Schmid factor 0.471), the activation free energy is less sensitive to the applied stress, leading to a smaller activation volume compared with the case of homogeneous nucleation (see Appendix F for more discussions on the activation volume).

V. DISCUSSION

A. Testing the “thermodynamic compensation law”

With the numerical results of $G_c(\sigma, T)$, we can test the approximations $S_c(\sigma) = H_c(\sigma)/T^*$ and $S_c(\gamma) = E_c(\gamma)/T^*$. Specifically, we are interested in whether $S_c(\sigma)$ is proportional to $H_c(\sigma)$, and whether $S_c(\gamma)$ is proportional to $E_c(\gamma)$, and if so, how the coefficient T^* compares with the (bulk or surface) melting point of Cu. While Eqs. (31) and (33) assume that the activation entropies do not depend on temperature, our data show that they do vary with temperature for $T \geq 400$ K. Hence, we test the average activation entropy \overline{S}_c in the range of zero to 300 K. For homogeneous nucleation, we find that $S_c(\gamma)$ can be roughly approximated by $E_c(\gamma)/T^*$ with $T^* \approx 2700$ K as shown in Fig. 8 (a), while $S_c(\sigma)$ is not proportional to $H_c(\sigma)$ as shown in Fig. 8 (c). On the other hand, for heterogeneous nucleation, we find that $S_c(\epsilon)$ can be approximately fitted to $E_c(\gamma)/T^*$ with $T^* = 2450$ K as shown in Fig. 8 (b), while $S_c(\sigma)$ can be approximately fitted to $H_c(\sigma)/T^*$ with $T^* = 930$ K as shown in

Fig. 8 (b). Both values of the fitted T^* are different from the surface melting temperature¹⁴ of $T_m = 700$ K. The value of $T^* = 2450$ K also greatly exceeds the (bulk) melting point of Cu (1358 K⁶³). Hence the empirical fitting parameter T^* is most likely not connected to the melting phenomenon. Fig. 8 shows a consistent trend that the activation entropy increases as the activation enthalpy (or the activation energy) increases. The “compensation law” appears to hold for $S_c(\sigma)$ in heterogeneous nucleation and for $S_c(\gamma)$ in homogeneous nucleation, but it does not hold for $S_c(\sigma)$ in homogeneous dislocation nucleation.

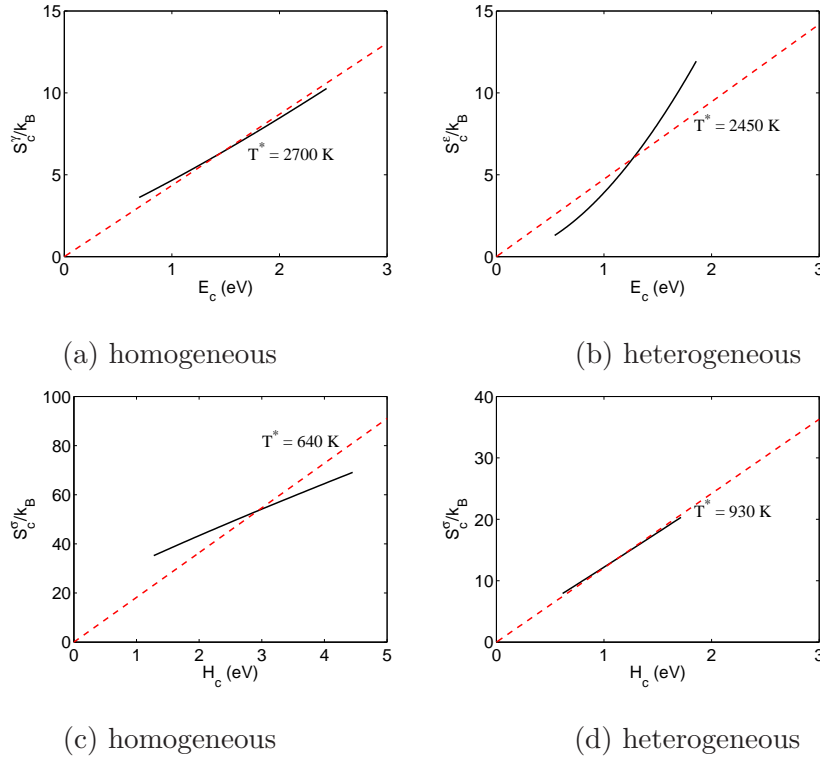


FIG. 8: The relation between E_c and S_c in the temperature range of zero to 300 K for (a) homogeneous and (b) heterogeneous nucleation. The relation between H_c and S_c for (c) homogeneous and (d) heterogeneous nucleation. The solid lines represent simulation data and the dashed lines are empirical fits of the form $S_c = E_c/T^*$ or $S_c = H_c/T^*$.

Because the activation entropies in dislocation nucleation mainly come from anharmonic effects such as thermal softening and thermal expansion, the exhibition of the “compensation law” in Fig. 8(a) and (d) cannot be attributed to the usual explanation^{46,62} that the activation energy is provided by multiple (small) excitations. The breakdown of the “compensation law” for $S_c(\sigma)$ in homogeneous dislocation nucleation is probably caused by the

elastic non-linearity at the high stress needed for homogeneous nucleation.

We note that the empirically fitted value of $T^* = E_c(\gamma)/S_c(\gamma)$ is close to the estimated value of 3000 K, which is based on a 10% reduction of the shear modulus as temperature increases from zero to 300 K (See Section IID). Therefore, Eq. (32) can be considered as a reasonable approximation to the activation Helmholtz free energy as a function of strain, i.e.

$$F_c(\gamma, T) \approx E_c(\gamma) \frac{\mu(T)}{\mu(0)} \quad (37)$$

whereas Eq. (28) is not a good approximation for $G_c(\sigma, T)$. In other words, Eq. (33) can be considered as a reasonable approximation to the activation entropy $S_c(\gamma)$, i.e.

$$S_c(\gamma) \approx -\frac{E_c(\gamma)}{\mu(0)} \frac{\partial \mu}{\partial T} \quad (38)$$

whereas Eq. (31) is not a good approximation for $S_c(\sigma)$. See Appendix D for more discussions on the approximation of $S_c(\sigma)$.

B. Entropic Effect on Nucleation Rate and Yield Strength

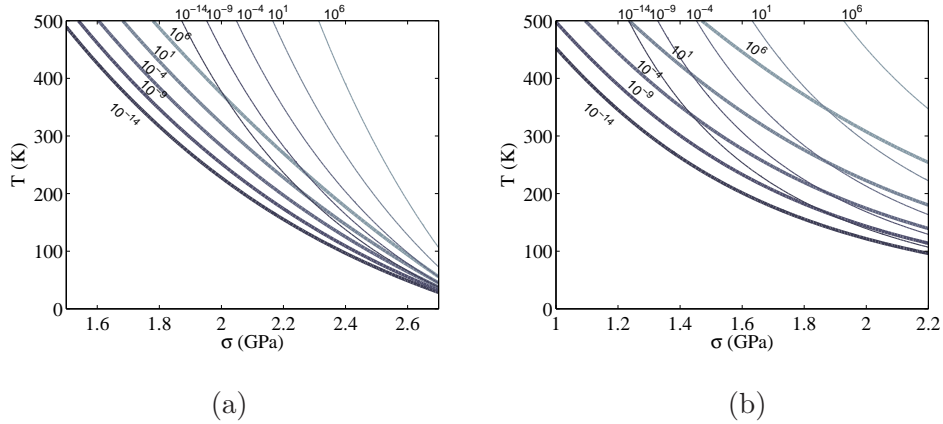


FIG. 9: Contour lines of (a) homogeneous and (b) heterogeneous dislocation nucleation rate per site I as a function of T and σ . The predictions with and without accounting for the activation entropy $S_c(\sigma)$ are plotted in thick and thin lines, respectively. The nucleation rate of $I \sim 10^6 \text{ s}^{-1}$ per site is accessible in typical MD timescales whereas the nucleation rate of $I \sim 10^{-4} - 10^{-9}$ is accessible in typical experimental timescales, depending on the number of nucleation sites.

In this section, we discuss how do the activation entropies affect experimental measurements. The simplest case to consider is to subject a perfect crystal to a constant stress (i.e. creep) loading condition and measure the rate of dislocation as a function of stress and temperature. (In practice, these kind of experiments are very difficult to carry out⁵, especially to observe homogeneous nucleation.) The data can be plotted in the form of contour lines, similar to those shown in Fig. 9, which are our theoretical predictions. To make these predictions, we use the activation Gibbs free energy obtained from umbrella sampling. Because the frequency prefactor $\nu_0 = f_c^+ \Gamma$ varies slowly with σ and T , we use average value $2.5 \times 10^{13} \text{ s}^{-1}$ for the homogeneous nucleation and $0.5 \times 10^{13} \text{ s}^{-1}$ for the heterogeneous nucleation. To show the physical effect of the large activation entropies, the thin lines plot the rate predictions if the effect of $S_c(\sigma)$ were completely neglected. Significant deviations between the two sets of contour lines are observed. For homogeneous dislocation nucleation, at $T = 400 \text{ K}$ and $\sigma_{xy} = 2.0 \text{ GPa}$ (where a thick and a thin contour line cross), we see about 20 orders of magnitude difference between the two contours. The difference between thick and thin curves becomes larger at smaller stress because activation entropy becomes larger at smaller stress. For heterogeneous nucleation, at $T = 300 \text{ K}$ and $\sigma_{zz} = 1.5 \text{ GPa}$, the neglect of activation entropy would cause an underestimate of the nucleation rate by 10 orders of magnitude. The smaller activation volume in heterogeneous dislocation is manifested by the larger gaps between the contour lines at different nucleation rates.

Experimentally, it is often convenient to impose a constant strain rate to the crystal and measure the stress-strain curve and the yield strength under the given strain rate. If the crystal contains no pre-existing defects, then the yield strength is the stress at which the first dislocation nucleates. The following implicit equation for the yield strength σ_Y has been derived by considering a nano-rod is loaded at a constant strain rate $\dot{\epsilon}$.

$$\frac{G_c(\sigma_Y, T)}{k_B T} = \ln \frac{k_B T N_s \nu_0}{E \dot{\epsilon} \Omega_c(\sigma_Y, T)} \quad (39)$$

This equation is derived^{14,57} based on the assumption that the nano-rod remains linear elastic with Young's modulus E prior to yielding and that ν_0 is insensitive to σ and T . One may apply this equation to homogeneous nucleation case if we replace E by the shear modulus μ and the uniaxial strain rate $\dot{\epsilon}$ by $\dot{\gamma}$. However, since we observe that the crystal becomes non-linear elastic prior to dislocation nucleation (see Fig. 2), we predict the yield strength numerically without assuming linear elasticity. The stress-strain relations shown in Fig. 2(b)

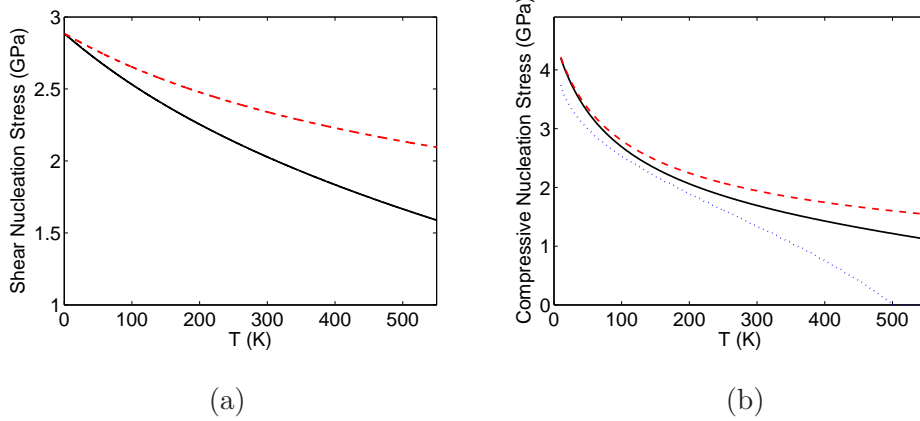


FIG. 10: (a) Nucleation stress of our bulk sample (containing 14,976 atoms) under constant shear strain loading rate $\dot{\gamma} = 10^{-3}$ and (b) nucleation stress of the nanorod under constant compressive strain loading rate $\dot{\epsilon} = 10^{-3}$. The strain rate 10^{-3} is experimentally accessible loading rate. The solid lines are the prediction based on the activation free energy computed by umbrella sampling. The dashed lines are the nucleation stress prediction when the activation entropy is neglected. The dotted line in (b) is the prediction based on the approximation by Zhu et al.¹⁴.

and (d) are used to extract the stress rate given the imposed strain rate and current strain. We replace E in Eq. (39) by $\partial\sigma/\partial\epsilon|_{\sigma=\sigma_Y}$. The athermal nucleation stress causing dislocation nucleation at $T = 0$ K is $\sigma_{xy} = 2.8$ GPa for homogeneous nucleation and $\sigma_{zz} = 4.7$ GPa for heterogeneous nucleation, which can also be obtained from in Fig. 2(b) and (d). At 300 K and a strain rate of 10^{-3} s^{-1} , however, the yield strength (i.e. nucleation stress) becomes $\sigma_{xy}^{\text{nuc}} = 2.0$ GPa for homogeneous nucleation, about 71% of the athermal nucleation stress, and $\sigma_{zz}^{\text{nuc}} = 1.7$ GPa for heterogeneous nucleation, about 36% of the athermal stress.

Fig. 10 plots our predictions of the yield strength as a function of temperature at a strain rate of 10^{-3} s^{-1} . As temperature rises, the nucleation stress decreases. This decrease is faster in the heterogeneous nucleation, Fig. 10(b), than in the homogeneous nucleation, Fig. 10(a). This observation can be explained by the larger activation volumes in the homogeneous nucleation than those in the heterogeneous nucleation. We note that the predicted nucleation stress depends on both the number of atoms in the sample and the applied strain rate. Increasing the number of atoms has the same effect as decreasing the strain rate.

For comparison, Fig. 10(b) also plots the prediction by Zhu et al.¹⁴, which is based on the assumption of $S_c(\sigma) = H_c(\sigma)/T_m$ with $T_m = 700$ K. (The yield strength is only plotted

up to $T = 300$ K in the original paper¹⁴.) The two predictions (solid and dotted line) are close to each other for $T < 200$ K, but their difference becomes large for $T \geq 300$ K. While the dotted line suggests that the yield strength vanishes at $T = 500$ K, our prediction (solid line) shows that the nanorod still retains 71% of its room temperature strength at 500 K. We believe this difference is caused by the overestimate of the activation entropy when assuming $T_m = 700$ K in $S_c(\sigma) = H_c(\sigma)/T_m$.

VI. SUMMARY

In this paper, we have shown that the dislocation nucleation rate is independent of whether a constant stress or a constant strain is applied, because $F_c(\gamma, T) = G_c(\sigma, T)$ when σ and γ lie on the stress-strain curve at temperature T . This naturally results in different activation entropies depending on whether constant stress or constant strain ensemble is used. The difference between the two activation entropies equals the activation volume times a term that characterizes the thermal softening effect. We have shown that the Becker-Döring theory combined with the activation free energy determined by umbrella sampling can accurately predict the rate of dislocation nucleation. In both homogeneous and heterogeneous dislocation nucleation, a large activation entropy at constant elastic strain is observed, and is attributed to the weakening of atomic bonds due to thermal expansion. The activation entropy at constant stress is even larger due to the thermal softening. Both effects are anharmonic in nature, and emphasize the need to go beyond harmonic approximation in the application of rate theories in solids. The “compensation law” turns out not to hold for homogeneous dislocation nucleation, probably because of the non-linear effects at high stress conditions. The “compensation law” appears to work better for heterogeneous nucleation, probably related to the linearity of the stress-strain relation. We have predicted that the yield stress decreases faster with temperature for the heterogeneous nucleation than for the homogeneous nucleation. We believe that our methods and the general conclusions are applicable to a wide range of nucleation processes in solids that are driven by shear stress, including cross slip, twinning and martensitic phase transformation.

APPENDIX A: EQUALITY OF CRITICAL SIZES n_c^σ AND n_c^γ

Suppose that the Gibbs free energy $G(n, \sigma, T)$ is maximized at $n = n_c^\sigma$, then

$$\left. \frac{\partial G(n, \sigma, T)}{\partial n} \right|_{\sigma, n=n_c^\sigma} = 0. \quad (\text{A1})$$

T is held constant throughout this section. Through Legendre transform, Eq. (5), we have the following property for the Helmholtz free energy $F(n, \gamma, T)$

$$\begin{aligned} \left. \frac{\partial F(n, \gamma, T)}{\partial n} \right|_{\gamma, n=n_c^\sigma} &= \left. \frac{\partial}{\partial n} \right|_{\gamma, n=n_c^\sigma} [G(n, \sigma, T) + \sigma\gamma V] \\ &= \left. \frac{\partial G(n, \sigma, T)}{\partial n} \right|_{\sigma, n=n_c^\sigma} + \left. \frac{\partial G(n, \sigma, T)}{\partial \sigma} \right|_{n=n_c^\sigma} \frac{\partial \sigma}{\partial n} + \frac{\partial \sigma}{\partial n} \gamma V \\ &= 0 - (V\gamma) \frac{\partial \sigma}{\partial n} + (V\gamma) \frac{\partial \sigma}{\partial n} = 0. \end{aligned} \quad (\text{A2})$$

By definition, $F(n, \gamma, T)$ reaches maximum at $n = n_c^\gamma$ at constant γ and T ,

$$\left. \frac{\partial F_c(n, \gamma, T)}{\partial n} \right|_{\gamma, n=n_c^\gamma} = 0 \quad (\text{A3})$$

Therefore, we establish that $n_c^\gamma = n_c^\sigma$, i.e. the maximizer n_c^σ of $G(n, \sigma, T)$ is also the maximizer n_c^γ of $F(n, \gamma, T)$.

APPENDIX B: EQUALITY OF ACTIVATION GIBBS AND HELMHOLTZ FREE ENERGIES

The activation Gibbs free energy is the free energy difference between state 0: a perfect crystal, and state 1: a crystal containing a critical dislocation loop under a same shear stress σ . Because of the plastic shear deformation caused by dislocation loop, state 1 has a higher strain (γ) than the state 0 (γ_0). It has been shown that the maximizer n_c^σ of $G(n, \sigma, T)$ equals to the maximizer of n_c^γ of $F(n, \gamma, T)$ when σ equals $\sigma(n_c, \gamma, T)$, as defined in Eq. (6). Note that we keep σ to be the stress at n_c, γ , and T . Then at the same σ , but for $n = 0$, the strain becomes γ_0 . Hence, the activation Gibbs free energy barrier can be written as

$$\begin{aligned} G_c &= G(n_c, \sigma, T) - G(0, \sigma, T) \\ &= F(n_c, \gamma, T) - \sigma\gamma V - F(0, \gamma_0, T) + \sigma\gamma_0 V \end{aligned} \quad (\text{B1})$$

Notice that $F(n_c, \gamma, T)$ and $F(0, \gamma_0, T)$ do not correspond to the same strain state, so that their difference is not the activation Helmholtz free energy. To construct the activation Helmholtz free energy, we subtract and add the $F(0, \gamma, T)$ term in the right hand side,

$$\begin{aligned}
G_c &= F(n_c, \gamma, T) - F(0, \gamma, T) + F(0, \gamma, T) - F(0, \gamma_0, T) - V\sigma(\gamma - \gamma_0) \\
&\approx F_c + \left. \frac{\partial F}{\partial \gamma} \right|_{\gamma_0, V} (\gamma - \gamma_0) + \frac{1}{2} \left. \frac{\partial^2 F}{\partial \gamma^2} \right|_{\gamma_0, V} (\gamma - \gamma_0)^2 - \sigma(\gamma V - \gamma_0 V) \\
&= F_c + \frac{1}{2} \left. \frac{\partial^2 F}{\partial \gamma^2} \right|_{\gamma_0, V} (\gamma - \gamma_0)^2 \\
&= F_c + \frac{1}{2} V \left. \frac{\partial \sigma}{\partial \gamma} \right|_{\gamma_0, V} (\gamma - \gamma_0)^2 \tag{B2}
\end{aligned}$$

Notice that $\gamma V = -\partial G(n_c, \sigma, T)/\partial \sigma$ and $\gamma_0 V = -\partial G(0, \sigma, T)/\partial \sigma$. Then $(\gamma V - \gamma_0 V)$ is equivalent to $-\frac{\partial}{\partial \sigma}(G(n_c, \sigma, T) - G(0, \sigma, T)) = -\frac{\partial G_c}{\partial \sigma} \equiv \Omega_c$, i.e. the activation volume. By plugging $(\gamma - \gamma_0) = \Omega_c/V$ into the equation, we have

$$\begin{aligned}
G_c &= F_c + \frac{1}{2} \frac{1}{V} \left. \frac{\partial \sigma}{\partial \gamma} \right|_{\gamma_0, V} (\Omega_c)^2 + O(V^{-2}) \\
&= F_c + O(V^{-1}) \tag{B3}
\end{aligned}$$

In the thermodynamics limit ($V \rightarrow \infty$), we have $G_c = F_c$. Hence, the nucleation rate does not depend on whether the crystal is subjected to constant stress or constant strain loading. The equality allows us to compute the activation Gibbs free energy $G_c(\sigma, T)$ by combining the activation Helmholtz free energy $F_c(\gamma, T)$ and the stress-strain relations of the perfect crystal shown in Fig. 2 (b) and (d).

APPENDIX C: PHYSICAL INTERPRETATION OF ACTIVATION ENTROPY DIFFERENCE ΔS_c

It is well-known that the entropy is a thermodynamic stat variable that is independent of the ensemble of choice, i.e., $S(n, \gamma, T) \equiv \partial F(n, \gamma, T)/\partial T|_{n, \gamma}$ and $S(n, \sigma, T) \equiv \partial G(n, \sigma, T)/\partial T|_{n, \sigma}$ equal to each other as long as $\sigma = V^{-1} \partial F/\partial \gamma|_{n, T}$. At the same time, the activation entropy is just the entropy difference between the activated state and the metastable state, i.e., $S_c(\gamma, T) = S(n_c, \gamma, T) - S(0, \gamma, T)$ and $S_c(\sigma, T) = S(n_c, \sigma, T) - S(0, \sigma, T)$. If the entropies in two ensembles can equal each other, it may seem puzzling how the activation entropies can be different.

The resolution of this apparent paradox is that under the constant applied stress, the nucleation of a dislocation loop causes a strain increase. Let γ be the strain at the state defined by $n = n_c$, σ , and T , and γ_0 be the strain at the state defined by $n = 0$, σ , and T , then $\gamma > \gamma_0$. Hence, we have $S(n_c, \sigma, T) = S(n_c, \gamma, T)$ and $S(0, \sigma, T) = S(0, \gamma_0, T)$, but $S(0, \gamma, T) \neq S(0, \gamma_0, T)$.

$$\begin{aligned}
S_c(\sigma, T) &= S(n_c, \sigma, T) - S(0, \sigma, T) \\
&= S(n_c, \gamma, T) - S(0, \gamma_0, T) \\
&= S(n_c, \gamma, T) - S(0, \gamma, T) + S(0, \gamma, T) - S(0, \gamma_0, T) \\
&= S_c(\gamma, T) + S(0, \gamma, T) - S(0, \gamma_0, T)
\end{aligned} \tag{C1}$$

This shows that the activation entropy difference $\Delta S_c \equiv S_c(\sigma) - S_c(\gamma)$ equals to $S(0, \gamma, T) - S(0, \gamma_0, T)$, which is entropy difference of the perfect crystal at two slightly different strains.

In the limit of $V \rightarrow \infty$, because we expect $(\gamma - \gamma_0) \rightarrow 0$, we might reach a false conclusion that $\Delta S_c = (S(0, \gamma, T) - S(0, \gamma_0, T)) \rightarrow 0$. Instead, the correct behavior in the thermodynamic limit can be obtained by expanding ΔS_c in a Taylor series.

$$\begin{aligned}
S(\gamma) - S(\gamma_0) &= \frac{\partial S}{\partial \gamma}(\gamma - \gamma_0) + \dots \\
&= - \left. \frac{\partial \sigma}{\partial T} \right|_{\gamma, V} V(\gamma - \gamma_0) + \dots
\end{aligned} \tag{C2}$$

where the Maxwell relationship $\partial S / \partial \gamma|_T = -V \partial \sigma / \partial T|_{\gamma, V}$ is used. The term $(\gamma V - \gamma_0 V)$ equals the activation volume Ω_c , and can be interpreted as plastic strain γ^{pl} due to formation of dislocation loop times the volume of the crystal, i.e.

$$(\gamma V - \gamma_0 V) = \Omega_c = \gamma^{pl} V = b A_c \tag{C3}$$

where b is the magnitude of the Burgers vector and A_c is the area of the critical dislocation loop. Using the relation $(\gamma - \gamma_0) = \Omega_c / V$, we have

$$\Delta S_c = S(\gamma) - S(\gamma_0) = - \left. \frac{\partial \sigma}{\partial T} \right|_{\gamma, V} \Omega_c + O(V^{-1}) \tag{C4}$$

which is exactly the same as Eq. (24).

A similar expression has been obtained for the difference between point defect formation entropies under constant pressure (S_p) and under constant volume (S_v)³⁹, with

$$S_p - S_v = \beta B V_{\text{rel}} \tag{C5}$$

where $\beta \equiv V^{-1} \left. \frac{\partial V}{\partial T} \right|_{p=0}$ is the thermal expansion factor at zero hydrostatic pressure p , B is the isothermal bulk modulus, and V_{rel} is the relaxation volume of the defect. In Cu, the value of $S_p - S_v$ is estimated to be $-1.7 k_B$ for a vacancy and $13.7 k_B$ for an interstitial³⁹. Comparing Eq. (C5) with Eq. (C4), we note that relaxation volume V_{rel} for point defects corresponds to the activation volume Ω for dislocation nucleation, and that βB corresponds to the $-\frac{\partial \sigma}{\partial T}$ term. The similarity between these two equations stems from the fact that they both express the entropy difference between two states, and the choice of the two states depends on whether the stress or the strain is kept constant when the defect is introduced. On the other hand, there are also some differences between the physics expressed by these two equations. First, thermal expansion plays a prominent role in Eq. (C5) because it focuses on hydrostatic stress and strain effects. In comparison, thermal expansion does not play a role in Eq. (C4) because it focuses on shear stress and strain effects. Second, the formation entropy of a point defect is the entropy difference between two metastable states and governs equilibrium properties, e.g. density of vacancies at thermal equilibrium. In comparison, the activation entropy is the entropy difference between a saddle (i.e. unstable) state and a metastable state and governs kinetics, such as dislocation nucleation rate. In addition, the saddle state (i.e. the size of the critical nucleus) depends on stress and temperature, while such complexity does not arise in the formation entropy of point defects.

APPENDIX D: APPROXIMATION OF $S_c(\sigma)$

In this appendix, we introduce a series of simplifying approximations to estimate the magnitude of $S_c(\sigma)$ in the low temperature, low stress limit. In the temperature range of zero to 300 K, the activation entropy is found to be insensitive to temperature. Starting from Eqs. (24) and (38), we have

$$S_c(\sigma) = S_c(\gamma) + \Delta S_c \approx -\frac{E_c(\gamma)}{\mu(0)} \frac{\partial \mu}{\partial T} - \Omega_c \left. \frac{\partial \sigma}{\partial T} \right|_{\gamma} \quad (\text{D1})$$

If we assume the crystal is linear elastic, i.e. $\sigma = \mu \gamma$, then,

$$S_c(\sigma) \approx -\frac{H_c(\sigma) + \Omega_c(\sigma) \cdot \sigma}{\mu(0)} \frac{\partial \mu}{\partial T} \quad (\text{D2})$$

Similar expressions can be obtained for normal (compressive) loading by replacing γ with ϵ and replacing μ by the Young's modulus.

To gain more intuition, we note that in the limit of $\sigma \rightarrow 0$, the line tension model³⁶ estimates that $H_c(\sigma) \propto \sigma^{-1}$. In addition, in the limit of $T \rightarrow 0$, $\Omega_c(\sigma) \approx -\partial H_c/\partial\sigma$. Under these conditions, $\Omega_c(\sigma) \cdot \sigma \approx H_c(\sigma)$, so that,

$$S_c(\sigma) \approx -\frac{2H_c(\sigma)}{\mu(0)} \frac{\partial\mu}{\partial T} \quad (\text{D3})$$

Comparing Eq. (D3) with Eq. (38), we have,

$$\frac{S_c(\sigma)}{H_c(\sigma)} \approx 2 \frac{S_c(\gamma)}{E_c(\gamma)} \quad (\text{D4})$$

This trend is qualitatively observed in heterogeneous nucleation, when comparing Fig. 8(b) and (d), and is less clear in homogeneous nucleation, when comparing Fig. 8(a) and (c). This is probably because the stress-strain relationship is more nonlinear in the case of homogeneous nucleation.

APPENDIX E: ACTIVATION FREE ENERGY DATA

In Table I and II, we provide the activation free energy data at all temperature and strain conditions in this study so that interested readers can use them as a benchmark. For homogeneous nucleation, the strain γ_{xy} is defined as $\Delta x/h_y^0$ where Δx is the displacement of the repeat vector initially in the y -direction along the x axis at each pure shear stress condition, and h_y^0 is the height of the cell along the y -axis at zero temperature without external loading. Shear stress σ_{xy} is determined from the x - y component of the average Virial stress. For heterogeneous nucleation, we take only the elastic strain into account. The elastic strain ϵ_{zz} at T is defined as $[L_z(\sigma, T) - L_z(\sigma = 0, T)]/L_z^0$ where $L_z(\sigma, T)$ is the length of the repeat vector along the z -axis, $L_z(\sigma = 0, T)$ is the equilibrium length at temperature T under zero stress. $L_z^0 = 20a_0 = 72.3\text{\AA}$ is the reference length (before relaxation), where a_0 is the lattice constant of copper. The compressional stress σ_{zz} is defined by $\sigma_{zz} = \langle F \rangle/d^2$ where $\langle F \rangle$ is the axial force computed from the z - z component of the average Virial stress, and $d = 15a_0 = 54.225\text{\AA}$ is the reference side length of the nanorod.

T	γ_{xy}	0.092	0.095	0.100	0.105	0.110	0.115	0.120	0.125	0.130	0.135	0.140	0.145
0 K	σ_{xy}	2.00	2.04	2.11	2.17	2.24	2.30	2.36	2.42	2.48	2.53	2.58	2.63
	E_c	2.2851	2.0866	1.7946	1.5426	1.3234	1.1315	0.9627	0.8133	0.6815	0.5648	0.4615	0.3703
100 K	σ_{xy}	1.94	1.98	2.05	2.11	2.17	2.22	2.28	2.33	2.38			
	\tilde{E}_c	2.196	2.004	1.718	1.477	1.268	1.085	0.925	0.784	0.660			
200 K	σ_{xy}	1.87	1.91	1.97	2.03	2.08	2.13	2.18	2.22				
	\tilde{E}_c	2.116	1.924	1.650	1.419	1.216	1.043	0.890	0.757				
	F_c	2.115	1.911	1.650	1.428	1.214	1.027	0.863	0.755				
	Γ	0.062	0.064	0.067	0.070	0.072	0.073	0.073	0.073				
	f_c^+	3.2	3.6	2.9	3.9	3.5	3.4	2.7	2.5				
300 K	σ_{xy}	1.80	1.83	1.89	1.94	1.98	2.02	2.06	2.10				
	\tilde{E}_c	2.042	1.853	1.586	1.362	1.171	1.004	0.859	0.730				
	F_c	2.054	1.876	1.585	1.370	1.173	1.006	0.860	0.728				
	Γ	0.048	0.049	0.051	0.054	0.056	0.056	0.055	0.054				
	f_c^+	3.6	4.5	5.1	3.6	4.4	4.2	5.1	4.4				
400 K	σ_{xy}	1.71	1.74	1.79	1.84	1.88	1.91	1.95					
	\tilde{E}_c	1.968	1.793	1.529	1.312	1.124	0.962	0.824					
	F_c	2.008	1.828	1.579	1.347	1.155	0.995	0.853					
	Γ	0.039	0.040	0.043	0.044	0.045	0.045	0.045					
	f_c^+	5.0	5.9	6.4	7.4	5.3	6.9	6.9					
500 K	σ_{xy}	1.62	1.64	1.69	1.73	1.76	1.79						
	\tilde{E}_c	1.897	1.727	1.476	1.261	1.081	0.925						
	F_c	1.939	1.782	1.548	1.341	1.167	1.010						
	Γ	0.034	0.035	0.037	0.038	0.038	0.038						
	f_c^+	7.7	6.6	8.3	9.9	7.0	7.3						

TABLE I: Data for homogeneous nucleation: σ_{xy} in GPa, E_c , \tilde{E}_c and F_c in eV, f_c^+ in 10^{14} s^{-1} . γ_{xy} and Γ are dimensionless. The error in \tilde{E}_c is about 0.003 eV, due to the small errors in equilibrating the simulation cell to achieve the pure shear stress state. The error in F_c is about $0.5 k_B T$, i.e. approximately 0.01 eV, due to the statistical error in umbrella sampling. The error in Zeldovich factor Γ is within ± 0.01 . The attachment rate f_c^+ has relative error of $\pm 50\%$.

APPENDIX F: ACTIVATION VOLUME AND CRITICAL LOOP SIZE

The activation volume Ω_c is defined as the derivative of activation free energy with stress, i.e., $\Omega_c(\sigma, T) = -\partial G_c / \partial \sigma|_T$, and measures the sensitivity of nucleation rate to the stress. Physically, it is interpreted as plastic strain associated with the dislocation loop times the volume of the crystal, i.e. $\Omega_c = bA_c$ where A_c is the area of critical dislocation loop (See Appendix C). In this appendix, we use our numerical data to test the validity of the latter interpretation.

$T = 0$ K	ϵ_{zz}	0.0303	0.0353	0.0403	0.0453	0.0503	0.0553	0.0603	0.0653	0.0703	0.0753	0.0803
	σ_{xy}	1.56	1.81	2.04	2.28	2.50	2.73	2.95	3.16	3.37	3.58	3.78
	E_c	1.5110	1.0383	0.7550	0.5650	0.4296	0.3277	0.2495	0.1878	0.1388	0.0993	0.0671
200 K	ϵ_{zz}	0.0312	0.0342	0.0372	0.0402	0.0432						
	σ_{xy}	1.56	1.69	1.82	1.95	2.07						
	F_c	1.278	1.017	0.825	0.690	0.571						
	Γ	0.030	0.038	0.047	0.054	0.062						
	f_c^+	1.1	1.0	0.91	0.84	0.85						
300 K	ϵ_{zz}	0.0307	0.0337	0.0367	0.0397	0.0427						
	σ_{xy}	1.48	1.60	1.72	1.83	1.94						
	F_c	1.254	1.004	0.824	0.695	0.579						
	Γ	0.021	0.028	0.033	0.045	0.049						
	f_c^+	1.5	1.4	1.3	1.1	1.1						
400 K	ϵ_{zz}	0.0301	0.0331	0.0361	0.0391	0.0421						
	σ_{xy}	1.39	1.50	1.62	1.73	1.83						
	F_c	1.258	1.003	0.839	0.700	0.578						
	Γ	0.019	0.028	0.029	0.037	0.038						
	f_c^+	1.8	1.8	1.7	1.5	1.4						
500 K	ϵ_{zz}	0.0296	0.0326	0.0356	0.0386							
	σ_{xy}	1.29	1.40	1.50	1.60							
	F_c	1.226	1.008	0.833	0.697							
	Γ	0.018	0.021	0.026	0.032							
	f_c^+	2.6	2.0	2.0	2.0							

TABLE II: Data for heterogeneous nucleation: σ_{zz} in GPa, E_c , and F_c in eV, f_c^+ in 10^{14} s^{-1} . γ_{xy} and Γ are dimensionless. The error in F_c is about $0.5 k_B T$, i.e. approximately 0.01 eV, due to the statistical error in umbrella sampling. The error in Zeldovich factor Γ is within ± 0.01 . The attachment rate f_c^+ has relative error of $\pm 50\%$. Notice that, due to the existence of thermal strain, the elastic strain values are slightly different at different temperatures.

Because the activation volume measures the sensitivity of $G_c(\sigma, T)$ to applied stress, see Eq. (10), it must be proportional to the Schmid factor, S , in uniaxial loading. Hence, the hypothesis we wish to test is,

$$\Omega_c = n_c b A_a S \quad (\text{F1})$$

where b is the magnitude of Burgers vector, A_a is the average area each atom occupy on the $\{111\}$ slip plane. Given that the lattice constant of Cu is $a_0 = 3.615 \text{ \AA}$, we have $b = a_0/\sqrt{6} = 1.48 \text{ \AA}$ and $A_a = \sqrt{6}a_0^2/4 = 5.66 \text{ \AA}^2$, so that $b A_a = 8.35 \text{ \AA}^3$. For the pure shear loading in our homogeneous nucleation case, the Schmid factor $S = 1$. For the uniaxial loading in our heterogeneous nucleation case, $S = 0.471$.

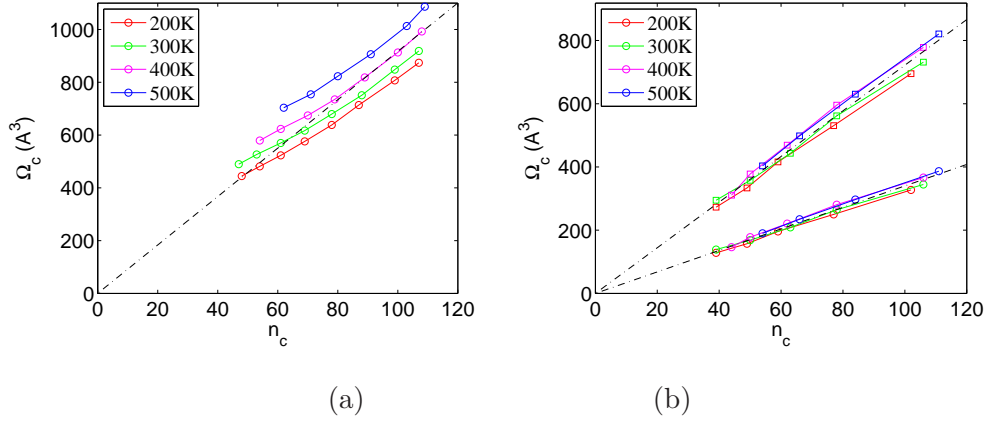


FIG. 11: The relation between critical dislocation size n_c and the activation volume $\Omega_c \equiv -\frac{\partial G_c}{\partial \sigma}$. (a) homogeneous nucleation (b) heterogeneous nucleation. Circles represent the activation volume obtained from the derivative of G_c with respect to σ . Squares represent the activation volume data multiplied by $1/S$ where S is the Schmid factor. Dashed lines are linear fits to the data.

Fig. 11 plots n_c versus Ω_c for both homogeneous and heterogeneous dislocation nucleation. In both cases, Ω_c appears to be roughly linear with n_c , as expected from Eq. (F1). For homogeneous nucleations under pure shear, Fig. 11(a), the slope of the curves is roughly $\Omega_c/n_c \approx 10 \text{\AA}^3$, close to the expected value of 8.35\AA^3 . For heterogeneous nucleation under compression, Fig. 11(b), the slopes of the curves after correction for the Schmid factor is roughly $\Omega_c/(n_c S) \approx 8 \text{\AA}^3$, which is similar to the case of homogeneous nucleation. Therefore, our data confirms that the idea that the activation volume is proportional to the size of the critical dislocation loop. The fact that $\Omega_c/(n_c S)$ is somewhat smaller than $b A_a$ supports the notion that the Burgers vector of a critical dislocation nucleus is smaller than that of a fully formed dislocation^{9,11}.

¹ X. Li, Y. Wei, L. Lu, K. Lu, and H. Gao: Dislocation nucleation governed softening and maximum strength in nano-twinned metals. *Nature* 464, 877 (2010).

² J. Li: The mechanics and physics of defect nucleation. *MRS Bull.* 32, 151 (2007).

³ T. Zhu, J. Li, S. Ogata, and S. Yip: Mechanics of ultra-strength materials. *MRS Bull.* 34, 167 (2009).

- ⁴ J. Li, K. J. Van Vliet, T. Zhu, S. Yip, and S. Suresh: Atomistic mechanisms governing elastic limit and incipient plasticity in crystals. *Nature* 418, 307 (2002).
- ⁵ C. A. Schuh, J. K. Mason, and A. C. Lund: Quantitative insight into dislocation nucleation from high-temperature nanoindentation experiments. *Nature Mater.* 4, 617 (2005).
- ⁶ P. Schall, I. Cohen, D. A. Weitz and F. Spaepen: Visualizing dislocation nucleation by indenting colloidal crystals. *Nature* 440, 319 (2006).
- ⁷ W. D. Nix, J. R. Greer, G. Feng, and E. T. Lilleodden: Deformation at the nanometer and micrometer length scales: Effects of strain gradients and dislocation starvation *Thin Solid Films* 515, 315 (2007).
- ⁸ S. Izumi, H. Ohta, C. Takahashi, T. Suzuki, and H. Saka: Shuffle-set dislocation nucleation in semiconductor silicon device. *Philos. Mag. Lett.* 90, 707 (2010).
- ⁹ G. Xu, A. S. Argon, M. Ortiz: Critical configurations for dislocation nucleation from crack tips. *Philos. Mag. A* 75, 341 (1997).
- ¹⁰ F. Frank, Symposium on Plastic Deformation of Crystalline Solids, Carnegie Institute of Technology, Pittsburgh, PA, 1950, p. 89.
- ¹¹ S. Aubry, K. Kang, S. Ryu, and W. Cai: Energy barrier for homogeneous dislocation nucleation: Comparing atomistic and continuum models *Scripta Mater.* 64, 1043 (2011).
- ¹² M. A. Tschopp, D. E. Spearot, and D. L. McDowell: Atomistic simulations of homogeneous dislocation nucleation in single crystal copper *Modell Simul Mater Sci Eng* 15, 693 (2007).
- ¹³ E. M. Bringa et al: Shock deformation of face-centered-cubic metals on subnanosecond timescales *Nat. Mater.* 5, 805 (2006).
- ¹⁴ T. Zhu, J. Li, A. Samanta, A. Leach, and K. Gall: Temperature and Strain-Rate Dependence of Surface Dislocation Nucleation *Phys. Rev. Lett.* 100, 025502 (2008).
- ¹⁵ P. Hanggi, P. Talkner, and M. Borkovec: Reaction-rate theory: Fifty years after Kramers *Rev Mod Phys* 62, 251 (1990).
- ¹⁶ R. Becker and W Döring: The kinetic treatment of nuclear formation in supersaturated vapors *Ann. Phys. (Weinheim, Ger)* 24, 719 (1935).
- ¹⁷ H. Eyring: The activated complex in chemical reactions *J. Chem. Phys.* 3, 107 (1935).
- ¹⁸ G. H. Vineyard: Frequency factors and isotop effects in solid state rate processes. *J. Phys. Chem. Solids* 3, 121 (1957).
- ¹⁹ H. Jónsson, G. Mills, K. W. Jacobsen (1998) Nudged elastic band method for finding minimum

- energy paths of transitions., in *classical and quantum dynamics in condensed phase simulations*, Ed. B. J. Berne, G. Ciccotti and D. F. Coker (World Scientific) pp 385-404.
- ²⁰ A. F. Voter: Introduction to the Kinetic Monte Carlo Method (Springer), 2007.
- ²¹ C. Jin, W. Ren, Y. Xiang: Computing transition rates of thermally activated events in dislocation dynamics, *Script. Mater.* 62, 206 (2010).
- ²² D. Chandler: Introduction to Modern Statistical Mechanics, (Oxford University Press), 1987.
- ²³ W. E, W. Ren, Eric Vanden-Eijnden: String Method for the Study of Rare Events *Phys. Rev. B* 66, 052301 (2002).
- ²⁴ W. E, W. Ren, and E. Vanden-Eijnden: Finite Temperature String Method for the Study of Rare Events *J. Phys. Chem. B* 109, 6688 (2005).
- ²⁵ U. F. Kocks, A. S. Argon, and M. F. Ashby, *Progress in Materials Science* 19, 1 (1975).
- ²⁶ S. Ryu, K. Kang, and W. Cai: entropic effect on the rate of dislocation nucleation *Proc Natl Acad Sci USA* 108, 5174 (2011).
- ²⁷ D. Frenkel and B. Smit: *understanding molecular simulation: from algorithms to applications*, Academic Press, San Diego. (2002).
- ²⁸ Physical properties of crystals: their representation by tensors and matrices, J. F. Nye, Clarendon Press 1957.
- ²⁹ To be more precise, σ is the Cauchy stress, and γV is the conjugate variable to σ . We choose V to be the volume of a reference state, i.e. the state at $\sigma = 0$. Then γ is the logarithmic (or Hencky) strain relative to the reference state³⁰. Here, we are interested in the regime of $0 \leq \gamma \leq 20\%$, and the difference between the Hencky strain and the simple engineering strain is negligible. Hence, in the numerical test case, we are going to let γ be the engineering strain.
- ³⁰ H. Xiao, O. T. Bruhns, and A. Meyers, Logarithmic strain, logarithmic spin and logarithmic rate, *Acta Mechanica*, 124, 89105 (1997).
- ³¹ Here we are excluding the effect of thermal expansion, by always defining the strain relative to the zero stress state at temperature T . Even though most crystals exhibit thermal softening, exceptions do exist. For example C_{66} of α -quartz decreases with temperature³².
- ³² R. Bechmann, A. D. Ballato, T. J. Lukaszek: Higher-Order Temperature Coefficients of the Elastic Stiffnesses and Compliances of Alpha-Quartz, *Proceedings of the IRE*, 50, 1812 (1962).
- ³³ W. C. Overton Jr., J. Gaffney, Temperature Variation of the Elastic Constants of Cubic Elements. I. Copper, *Phys. Rev.* 98, 969 (1955).

- R. Bechmann, A. D. Ballato, T. J. Lukaszek: Higher-Order Temperature Coefficients of the Elastic Stiffnesses and Compliances of Alpha-Quartz, *Proceedings of the IRE*, 50, 1812 (1962).
- ³⁴ E. Whalley: Use of volumes of activation for determining reaction mechanisms. in *Advances in Physical Organic Chemistry*, V. Gold, ed., pp 93-162, Academic Press, London (1964).
- ³⁵ M. L. Tonnet and E. Whalley: Effect of pressure on the alkaline hydrolysis of ethyl acetate in acetone-water solutions. parameters of activation at constant volume. *Can. J. Chem.* 53, 3414 (1975).
- ³⁶ We can use the line tension model to give a rough estimate of the formation energy of a circular dislocation loop of radius r , i.e. $E_{\text{loop}} = 2\pi r\tau - b\pi r^2\sigma$, where τ is the dislocation line energy per unit length and b is the magnitude of Burgers vector. Maximizing E_{loop} with respect to r gives the energy barrier $E_c = \frac{\pi\tau^2}{b\sigma}$ at the critical radius $r_c = \frac{\tau}{b\sigma}$. The activation volume is $\Omega_c = b\pi r_c^2 = \frac{\pi\tau^2}{b\sigma^2}$, which diverges in the limit of $\sigma \rightarrow 0$.
- ³⁷ J. W. Cahn and F. R. N. Nabarro, Thermal activation under shear, *Philos. Mag. A* 81, 1409 (2001).
- ³⁸ A. H. Cottrell, Thermally activated plastic glide, *Philos. Mag. Lett.* 82, 65 (2002).
- ³⁹ Y. Mishin, M. R. Sorensen, and A. F. Voter, Calculation of point-defect entropy in metals, *Philos. Mag. A* 81, 2591 (2001).
- ⁴⁰ D. Gupta, ed: Diffusion Processes in Advanced Technological Materials, Springer, p.140 (2002).
- ⁴¹ C. Kittel: Introduction to Solid State Physics, Wiley, 8th ed (2004).
- ⁴² A. S. Argon, R. D. Andrews, J. A. Godrick, and W. Whitney: Plastic Deformation Bands in Glassy Polystyrene *J. Appl. Phys.* 39, 1899 (1968).
- ⁴³ R. J. DiMelfi, W. D. Nix, D. M. Barnett, J. H. Holbrook, and G. M. Pound: An Analysis of the Entropy of Thermally Activated Dislocation Motion Based on the Theory of Thermoelasticity *phys. stat. sol. (b)* 75, 573 (1976).
- ⁴⁴ R. J. DiMelfi, W. D. Nix, D. M. Barnett, and G. M. Pound: The equivalence of two methods for computing the activation entropy for dislocation motion. *Acta. Mater.* 28, 231 (1980).
- ⁴⁵ G. Kemeny and B. Rosenberg: Compensation law in thermodynamics and thermal death *Nature* 243, 400 (1973).
- ⁴⁶ A. Yelon, M. Movagha, and H. M. Branz: Origin and consequences of the compensation (Meyer-Neldel) law *Phy. Rev. B* 46, 12243 (1992).
- ⁴⁷ M. Born: Thermodynamics of Crystals and Melting *J. Chem. Phys.* 7, 591 (1939).

- ⁴⁸ S. Brochard, P. Hirel, L. Pizzagalli, and J. Godet: Elastic limit for surface step dislocation nucleation in face-centered cubic metals: Temperature and step height dependence *Acta Materialia* 58, 4182 (2010).
- ⁴⁹ M. Khantha, D. P. Pope and V. Vitek: Dislocation screening and the brittle-to-ductile transition: a Kosterlitz-Thouless type instability. *Phys. Rev. Lett.* 74, 684 (1994).
- ⁵⁰ Y. Mishin, M. J. Mehl, D. A. Papaconstantopoulos, A. F. Voter, and J. D. Kress: Structural stability and lattice defects in copper: ab initio, tight-binding, and embedded-atom calculations. *Phys. Rev. B.* 63, 224106 (2001).
- ⁵¹ J. P. Hirth and J. Lothe (1992). *Theory of Dislocations* (Krieger, New York)
- ⁵² M. Parrinello and A. Rahman: Crystal Structure and Pair Potentials: A Molecular Dynamics Study *Phys. Rev. Lett.* 45 1196 (1980).
- ⁵³ H. C. Anderson: Molecular dynamics at constant pressure and/or temperature *J. Chem. Phys.* 72, 2384 (1980).
- ⁵⁴ W. G. Hoover: Canonical Dynamics: Equilibrium Phase Space Distribution *Phys. Rev. A* 31, 1695 (1985).
- ⁵⁵ The activation Gibbs free energy at zero temperature, i.e. $G_c(\sigma, T = 0)$, can be obtained from the stress-controlled NEB method⁵⁶. Due to the finite size of the simulation cell, $G_c(\sigma, T = 0)$ is expected to be slightly different from $F_c(\gamma, T = 0)$ obtained under the constant strain condition, but such difference is ignored in this paper.
- ⁵⁶ T. Zhu, J. Li, K. J. Van Vliet, S. Ogata, S. Yip, and S. Suresh, *J. Mech. Phys. Sol.* 52, 691 (2004).
- ⁵⁷ A. H. W. Ngan, L. Zuo, and P. C. Wo Size dependence and stochastic nature of yield strength of micron-sized crystals: a case study on Ni₃Al. *Proc. Royal Soc. A* 462:1661-1681 (2006).
- ⁵⁸ T. Zhu, J. Li, A. Samanta, H. G. Kim, and S. Suresh: Interfacial plasticity governs strain rate sensitivity and ductility in nanostructured metals. *Proc. Natl. Acad. Sci. USA* 104, 3031 (2007).
- ⁵⁹ S. Ryu and W. Cai: Validity of classical nucleation theory for Ising models, *Phys. Rev. E* 81, 030601(R) (2010).
- ⁶⁰ S. M. Foiles: Evaluation of harmonic methods for calculating the free energy of defects in solids *Phys. Rev. B* 49, 14930 (1994).
- ⁶¹ M. de Koning, Caetano R. Miranda, and A. Antonelli: Atomistic prediction of equilibrium vacancy concentrations in Ni₃Al *Phys. Rev. B* 66, 104110 (2002).

- ⁶² A. Yelon, B. Movaghar, and R. S. Crandall: Multi-excitation entropy: its role in thermodynamics and kinetics *Rep. Prog. Phys.* 69, 1145 (2006).
- ⁶³ S. Ryu and W. Cai: Comparison of thermal properties predicted by interatomic potential models *Modelling Simul. Mater. Sci. Eng.* 16, 085005 (2008).